Spin implementation of the bosonic Kitaev chain

Meritxell Valls Boix

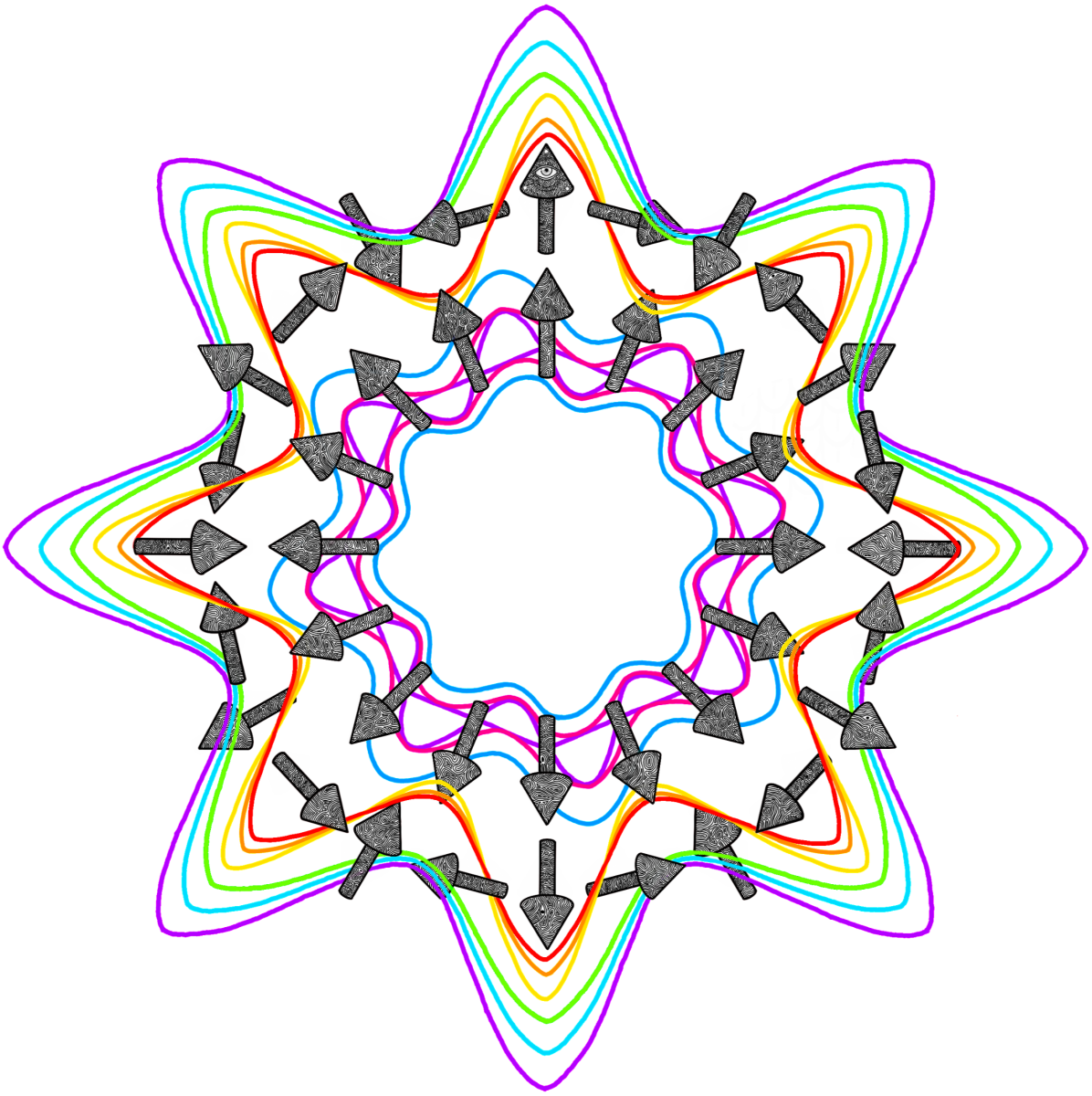

Supervisor: R.A. Duine
Daily supervisor: A. Asgharpour

Utrecht University
July 2nd, 2024

Contents

1 Introduction

1.1 Topology in physics

Topology is the matematical fields that allows for the classification of shapes. Two shapes are topologically equivalent, i.e. belong in the same topological class, if they can be deformed into each other by means of a continuous transformation such as stretching or twisting, but not making a cut or gluing. Topological classes are labelled by a number, known as the topological invariant, which is left unchanged by continuous transformations.
An intuitive example of topological groups is given by the number of holes in objects. Starting with a ring, we can stretch it into a straw or −with a bit of skill− it can be deformed into a tea cup, but it is impossible to obtain a pair of glassless glasses since that would require making an additional hole. Hence the ring, straw and tea cup are in the topological group labelled by the topological invariant, that is the number of holes, 1 and the glasses in the group labelled by a 2.
Nowadays topology has become a key tool in many fields of physics; from computational physics, which uses topological data analysis to extract information on the shape of the data [1, 2] to biophysics, which uses knot theory to characterise from a single protein to a whole chromosome [3].
Here we focus on the role of topology in condensed matter physics. Pioneered by David J. Thouless [4], J. Michael Kosterlitz [5, 6, 7] and F. Duncan M. Haldane [8, 9], who received the Nobel prize in 2016 for introducing topological concepts in condensed matter phyics. This allowed to gain a better understanding of phase transitions [10], superconductivity [11] and a long long list of interesting phenomena that arise when a system has a non-trivial topology[1] [12]. The topological invariants in this case are the winding number in real space, which counts how many times a closed curve goes around the origin, and the Chern number in momentum space, which measures whether there is an obstruction to chosing a global gauge.
A well known model with a non-trivial topology is the fermionic Kitaev chain (FKC), a toy model of a p-wave superconductor with a winding number equal to one that exhibits a pair of Majorana zero modes at both edges of the chain [13, 14]. The Majorana fermions are a kind of quasiparticle that satisfy two conditions: they satisfy the Dirac equation and they are their own anti-particle [11].
The emergence of Majorana modes in the FKC is a consequence of its topological nature; the low energy Hamiltonian of topological superconductors describes a linear dispersion that satisfies the Dirac equation. Moreover, in the superconducting phase there is particle-hole symmetry, hence both the conditions for the emergence of Majorana modes are satisfied [11, 15].

1.2 The Bosonic Kitaev chain

We now discuss some basic properties of the bosonic Kitaev chain (BKC) by following [16]. The BKC is a chain of non-interacting bosonic cavities subject to nearest-neighbour parametric driving that defines a model for a one-dimensional superconductor defined in analogy to the FKC. The BKC is defined in such a way that it exhibits the non-trivial topology from the fermionic case as

$$\hat{H}_B = \frac{1}{2}\sum_j \left(it\hat{a}^\dagger_{j+1}\hat{a}_j + i\Delta\hat{a}^\dagger_{j+1}\hat{a}^\dagger_j + \text{h.c.}\right), \tag{1}$$

where t is the hopping parameter and Δ is the driving amplitude. We now write the Hamiltonian in momentum space by taking the Fourier transform $\hat{a}_j = N^{-1/2}\sum_j e^{ikj}\hat{a}_k$ yielding

$$\hat{H}_B = \frac{1}{2}\sum_{k\in 1\text{BZ}} \hat{\vec{A}}^\dagger_k[\vec{h}_B(k)\cdot\hat{\vec{\sigma}}]\hat{\vec{A}}_k \tag{2}$$

with $\hat{\vec{A}}^\dagger_k = (\hat{a}^\dagger_k, \hat{a}_{-k})$, $\hat{\vec{\sigma}}$ the vector of Pauli matrices and $\vec{h}_B(k) = (0, -\Delta\cos(k), t\sin(k))$. Figure 1 shows that the vector $\vec{h}_B(k)$ winds once around the origin thus the BKC has a winding number equal to

[1] A system has a trivial topology when the topological invariant is zero and a non-trivial topology when the invariant is non-zero.

one. Due to the non-trivial topology of the model, the BKC exhibits a number of interesting properties.

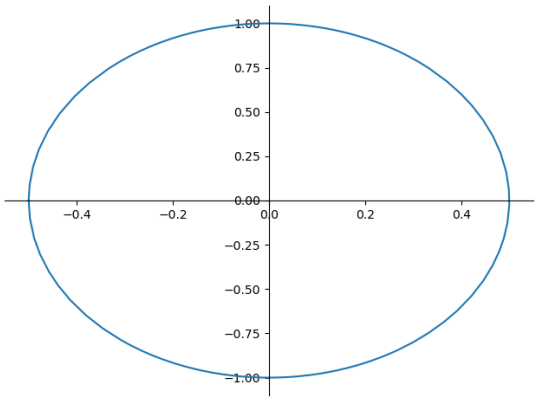

Figure 1: $\vec{h}_B(k)$ for $\Delta = t/2 = 0.5$. $\vec{h}_B$ winds once around the origin.

A more intuitive description of the BKC is obtained by defining it in terms of the Hermitian quadrature operators on each site [17]

$$\hat{x}_j = \frac{1}{\sqrt{2}}(\hat{a}_j^\dagger + \hat{a}_j), \tag{3a}$$

$$\hat{p}_j = \frac{i}{\sqrt{2}}(\hat{a}_j^\dagger - \hat{a}_j). \tag{3b}$$

These operators –which satisfy the canonical commutation relation $[\hat{x}_j, \hat{p}_{j'}] = i\delta_{j,j'}$– are used to describe the state of monochromatic light in terms of its amplitude and phase, with the $\hat{x}$ quadrature representing the in-phase component of the light field, which describes the amplitude of the field. The $\hat{p}$ quadrature then represents the out-of-phase component of the field and thus describes the phase of the light field. By writing Eq. (1) in terms of the quadratures the Hamiltonian becomes

$$\hat{H}_B = \frac{1}{2}\sum_j \left(-(t-\Delta)\hat{x}_{j+1}\hat{p}_j + (t+\Delta)\hat{p}_{j+1}\hat{x}_j\right), \tag{4}$$

and the asymmetry of our system is now obvious; the x-quadrature at site j is only coupled to the p-quadrature at the neighbouring sites in an asymmetric manner. As a result of this asymmetry, the BKC exhibits unusual propagation of excitations within the bulk which is not present in the FKC.

To see the consequences of the asymmetric coupling between the quadratures, we look at the Heisenberg equations of motion

$$\dot{\hat{x}}_j = \frac{t+\Delta}{2}\hat{x}_{j-1} - \frac{t-\Delta}{2}\hat{x}_{j+1}, \tag{5a}$$

$$\dot{\hat{p}}_j = \frac{t-\Delta}{2}\hat{p}_{j-1} - \frac{t+\Delta}{2}\hat{p}_{j+1}, \tag{5b}$$

where we see that the dynamics of the x-quadrature is completely independent of the p-quadrature and viceversa. Furthermore, each quadrature is forced in a spatially asymmetric fashion by its neighbours, showing a complete asymmetry in the limiting case where $t \to \Delta$. In this limit, the x-quadratures are only forced by their left neighbours, while the p-quadratures are only forced by their right neighbours, meaning that the transport of a wave packet in our lattice will be directional with the direction of propagation given by the phase of the wave packet. Moreover, an x-excitation will be amplified as it propagates to the right and deamplified as it propagates to the left whereas a p-excitation will exhibit the opposite behaviour, being amplified as it propagates to the left and deamplified as it propagates to the right.

Due to the directionality of our system, it is natural to ask whether or not our model is stable as it would be unphysical to allow for an infinite amplification of the excitations. Consequently, when we consider the case of periodic boundary conditions (PBC), our system would always be dynamically unstable since in this case an excitation could propagate in a given direction indefinetly leading to an infinite amplification.
In the case of open boundary conditions (OBC), by assuming $t > \Delta > 0$, the system is always dynamically stable and can be mapped to a particle conserving tight-binding chain. In contrast with PBC, the presence of edges in the chain ensures that the excitation cannot be indefinetly amplified. When an excitation reaches the edge of the chain, it changes direction while mantaining the same phase and is therefore deamplified.

1.3 This thesis

In this thesis, we aim to define a spin system such that its excitations propagate in the same way as quadratures do in the photonic BKC. To do so, we start by defining a spin Hamiltonian in Section 2 and determine its ground state (GS) in Section 3. The ground state corresponds to the stable configuration around which excitations propagate. We then map the spin system to the photonic one through a linear Holstein-Primakkof transformation in Section 4, by considering that the system is in its ground state and allow for small fluctuations, which correspond to the bosons of the photonic system. By doing so, we prove that in the ferromagnetic ground state, the system acts as the BKC with an additional constraint that changes the regime of stability of the chain. Moreover, we prove that the same spin Hamiltonian, gives rise to a new model when linearising around the non-collinear ground state in the absence of a magnetic field. At last we study the dynamics of the magnonic BKC in Section 5 and the new model in Section 6 by computing the equations of motion and dispersion relation.

2 Hamiltonian

As we will show in Section 4.1, the Hamiltonian that yields the BKC Eq. (1) when performing a Holstein-Primakkof transformation is

$$\hat{H} = \frac{\Delta}{2S}\sum_j \left(\hat{S}^x_{j+1}\hat{S}^y_j + \hat{S}^y_{j+1}\hat{S}^x_j\right) - \frac{t}{2S}\sum_j \left(\hat{S}^x_{j+1}\hat{S}^y_j - \hat{S}^y_{j+1}\hat{S}^x_j\right) - \frac{\mathrm{J}^z}{2}\sum_j \hat{S}^z_{j+1}\hat{S}^z_j - B\sum_{j=1}^{N}\hat{S}^z_j, \tag{6a}$$

$$\hat{H} = \frac{1}{2}\sum_j \left(-\vec{D}\cdot(\hat{\vec{S}}_{j+1}\times\hat{\vec{S}}_j) + \hat{\vec{S}}_{j+1}\underline{\Gamma}\hat{\vec{S}}_j - \frac{\mathrm{J}^z}{3}\hat{\vec{S}}_{j+1}\cdot\hat{\vec{S}}_j\right) - B\sum_{j=1}^{N}\hat{S}^z_j, \tag{6b}$$

where we have defined

$$\underline{\Gamma} = \begin{pmatrix} \mathrm{J}^z/3 & \Delta/S & 0 \\ \Delta/S & \mathrm{J}^z/3 & 0 \\ 0 & 0 & -2\mathrm{J}^z/3 \end{pmatrix}, \tag{7a}$$

$$\vec{D} = \left(0, 0, \frac{t}{S}\right). \tag{7b}$$

The Hamiltonian can be saparated into two parts corresponding to the isotropic and the anisotropic exchanges in addition to the magnetic field in the z-direction.
The isotropic exchange $\hat{H}_{isotropic} = -\mathrm{J}^z/3\sum_{\langle i,j\rangle}\hat{\vec{S}}_i\cdot\hat{\vec{S}}_j$, where we consider $\mathrm{J}^z > 0$, favours the parallel alignment of spins in the z-direction and is usually the dominant term. This term together with the magnetic field $-B\sum_j \hat{S}^z_j$ will ensure the stability of the ground state around which we will later linearize. The anisotropic exchange is separated into a symmetric and an antisymmetric part, the antisymmetric anisotropic interaction or Dzyaloshinskii-Moryia interaction (DMI) given by $\hat{H}_{DMI} = -\sum_{\langle i,j\rangle}\vec{D}\cdot(\hat{\vec{S}}_i\times\hat{\vec{S}}_j)$ with $\vec{D}$ the DM vector. The DMI arises from the mirror-reflection and inversion symmetry breaking and that stabilizes chiral spin textures. It is relativistic in nature, thus

its effect is usually weak. This interaction favours an alignment of spins that is neither parallel nor antiparallel and depends on the shape of the DM vector. In our case, since the DM vector is in the z-direction, the DMI favours the alignment of spins in the xy plane.

The symmetric anisotropic exchange, defined by $\hat{H}_{anisotropic} = \sum_{\langle i,j\rangle} \hat{\vec{S}}_i \underline{\Gamma} \hat{\vec{S}}_j$, and as is the case of the DMI, favours the missalignment of spins in the xy plane.

Throughout this thesis we consider nearest-neighbour interaction between the spins in the chain, which has a total number of sites N. Moreover, we consider two kinds of boundary conditions: the PBC, where we assume $\hat{\vec{S}}_{N+1} = \hat{\vec{S}}_1$ and the OBC, where $\hat{\vec{S}}_0 = \hat{\vec{S}}_{N+1} = \vec{0}$. To simplify the notation, we define

$$\mathcal{N} = \sum_{<i,j>} 1 = \begin{cases} N-1 & \text{for OBC,} \\ N & \text{for PBC.} \end{cases} \tag{8}$$

3 Ground state

Since we want to study the propagation of magnons in the chain, we must first compute the classical ground state of the system, which correspods to the lower energy state. The small fluctuations around the ground state then correspond to the bosons in the BKC.

In order to determine the GS of the system, it is useful to make the Hamiltonian real by getting rid of the $\pi/2$ phase through the gauge transformation $\hat{S}^{\pm} = e^{\pm i\pi j/2}\hat{S}^{\pm}$ which yieds

$$\hat{H} = \frac{S}{2}\sum_j [(t + (-1)^j\Delta)\hat{S}^x_j\hat{S}^x_{j+1} + (t - (-1)^j\Delta)\hat{S}^y_j\hat{S}^y_{j+1}] - \frac{J^z}{2}\sum_j \hat{S}^z_j\hat{S}^z_{j+1} - B\sum_{j=1}^{N}\hat{S}^z_j. \tag{9}$$

Next, we define the spin in spherical coordinates as $\hat{\vec{S}}_j = S(\sin\theta\cos\chi_j, \sin\theta\sin\chi_j, \cos\theta)$, where

$$\chi_j = \varphi_j - \frac{\pi}{2}j$$

is the gauged azimuthal angle. Then the Hamiltonian reads

$$\hat{H} = \frac{S}{2}\Phi\sin^2\theta - \frac{J^z S^2\mathcal{N}}{2}\cos^2\theta - BSN\cos\theta, \tag{10}$$

where we assume[2] homogeneity in θ, and where we defined the quantity

$$\Phi = \sum_j [(t + (-1)^j\Delta)\cos\chi_{j+1}\cos\chi_j + (t - (-1)^j\Delta)\sin\chi_{j+1}\sin\chi_j]. \tag{11}$$

Since $S\sin^2\theta \geq 0$ and Φ contains all the χ_j dependence of the Hamiltonian, the minima of $\hat{H}$ with respect to χ_j corresponds to the minima of Φ, which is given by

$$\begin{aligned} \frac{d\Phi}{d\chi_j} = &-[(t + (-1)^j\Delta)\cos\chi_{j+1} + (t - (-1)^j\Delta)\cos\chi_{j-1}]\sin\chi_j \\ &+ [(t - (-1)^j\Delta)\sin\chi_{j+1} + (t + (-1)^j\Delta)\sin\chi_{j-1}]\cos\chi_j = 0, \end{aligned} \tag{12a}$$

[2]We are allowed to do that because we already know the answer and this section would be way too long otherwise since we would not be able to use the compact notation Φ. Moreover, by noting that Eq. (9) corresponds to the Hamiltonian of the XYZ-chain, we know that $J^z > 0$ corresponds to a ferromagnetic alignment of spins, which is homogeneous in θ. If you still don't trust me –fair enough– you can try it yourelf.

$$\left.\frac{d^2\Phi}{d\chi_j^2}\right|_{\chi_{0,j}} = -[(t+(-1)^j\Delta)\cos\chi_{0,j+1} + (t-(-1)^j\Delta)\cos\chi_{0,j-1}]\cos\chi_{0,j} - [(t-(-1)^j\Delta)\sin\chi_{0,j+1} + (t+(-1)^j\Delta)\sin\chi_{0,j-1}]\sin\chi_{0,j} > 0, \tag{12b}$$

Eq. (12a) allows for two solutions

$$\cos\chi_j = 0 \ \ \forall j \ \ \Rightarrow \ \ \chi_{0,j}^{(1)} = \frac{\pi}{2}(2n_j+1), \tag{13a}$$

$$\sin\chi_j = 0 \ \ \forall j \ \ \Rightarrow \ \ \chi_{0,j}^{(2)} = \pi n_j \tag{13b}$$

where n_j is an integer with a site dependence determined by Eq. (12b), that is

$$\left.\frac{d^2\Phi}{d\chi_j^2}\right|_{\chi_{0,j}^{(1)}} = (-1)^{n_j+1}[(t-(-1)^j\Delta)(-1)^{n_{j+1}} + (t+(-1)^j\Delta)(-1)^{n_{j-1}}] > 0, \tag{14a}$$

$$\left.\frac{d^2\Phi}{d\chi_j^2}\right|_{\chi_{0,j}^{(2)}} = (-1)^{n_j+1}[(t+(-1)^j\Delta)(-1)^{n_{j+1}} + (t-(-1)^j\Delta)(-1)^{n_{j-1}}] > 0. \tag{14b}$$

This imposes that $n_j + n_{j\pm1} = 2m+1$ for $m \in \mathbb{Z}$, hence the n_j's must have alternating parity. In the case of PBC, we have $n_{N+1} = n_1$ thus n_N and n_1 must have opposite parities, which imposes that the total number of spins in the chain N has to be even[3].
The value of Φ at the minima is then given by

$$\Phi_0^{(1)} := \Phi|_{\chi_{0,j}^{(1)}} = \begin{cases} -(N-1)t - \Delta & \text{for OBC with N even,} \\ -(N-1)t & \text{for OBC with N odd,} \\ -Nt & \text{for PBC;} \end{cases} \tag{15a}$$

$$\Phi_0^{(2)} := \Phi|_{\chi_{0,j}^{(2)}} = \begin{cases} -(N-1)t + \Delta & \text{for N even,} \\ -(N-1)t & \text{for N odd,} \\ -Nt & \text{for PBC.} \end{cases} \tag{15b}$$

We note that when there is an even number of spacings, i.e. for PBC and OBC with an odd number of sites, the GS is independent of the driving amplitude Δ.
Next we minimize the Hamiltonian with respect to θ by solving the system of equations

$$\frac{\partial\hat{H}}{\partial\theta} = S\left(\Phi + J^z S\mathcal{N}\right)\cos\theta\sin\theta + BSN\sin\theta = 0, \tag{16a}$$

$$\left.\frac{\partial^2\hat{H}}{\partial\theta^2}\right|_{\theta_0,\chi_{0,j}} = S\left(\Phi_0 + J^z S\mathcal{N}\right)(\cos^2\theta_0 - \sin^2\theta_0) + BSN\cos\theta_0 > 0, \tag{16b}$$

where $\Phi_0 := \Phi|_{\chi_{0,j}}$ is strictly negative for any value of $\chi_{0,j}$. To find the minima with respect to θ, we will consider two cases: first, we look at the case where there is no magnetic field applied to the lattice and then we look at how the GS changes when a magnetic field in the z-direction is applied to the system.

[3]As we see below, the GS is made of a pattern of four spins, and so in the case of PBC we consider that the number of sites N is a multiple of four.

3.1 Ground state in zero magnetic field

In the absence of magnetic field, Eq. (16a) allows for two solutions given by

$$\cos\theta = 0 \;\Rightarrow\; \theta_0^{(1)} = \frac{\pi}{2}(2n+1), \tag{17a}$$

$$\sin\theta = 0 \;\Rightarrow\; \theta_0^{(2)} = \pi n, \tag{17b}$$

where $n \in \mathbb{Z}$. Eq. (16b) now leads to the regime of validity of each of the minima:

$$\left.\frac{\partial^2 \hat{H}}{\partial\theta^2}\right|_{\theta_0^{(1)},\chi_{0,j}} = -S\left(\Phi_0 + \mathrm{J}^z S\mathcal{N}\right) > 0 \;\Rightarrow\; \mathrm{J}^z S\mathcal{N} < |\Phi_0|, \tag{18a}$$

$$\left.\frac{\partial^2 \hat{H}}{\partial\theta^2}\right|_{\theta_0^{(2)},\chi_{0,j}} = S\left(\Phi_0 + \mathrm{J}^z S\mathcal{N}\right) > 0 \;\Rightarrow\; \mathrm{J}^z S\mathcal{N} > |\Phi_0|. \tag{18b}$$

The GS energy of the system is then given by

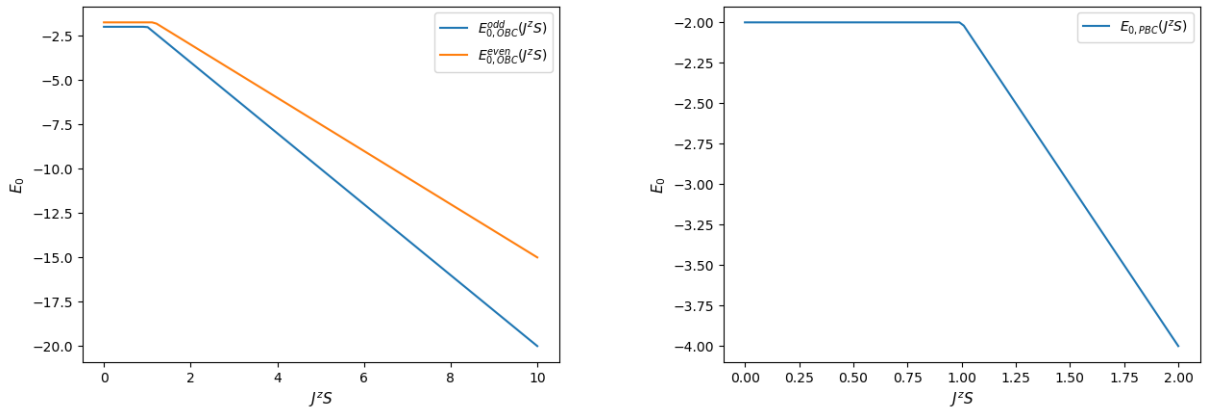

(a) (b)

Figure 2: Ground state energy of the chain as a function of the isotropic exchange parameter $\mathrm{J}^z S$ for $t = 1$, $\Delta = 0.5$ and $B = 0$. We observe a first order phase transition with the phase of the system determined by the dominant energy contribution. **(a)** Ground state energy for the chain with OBC in the case of an even number of sites ($N = 4$) and an odd number of sites ($N = 5$). **(b)** Ground state energy for the chain with PBC and $N = 4$.

$$E_{0,OBC}^{even} = \begin{cases} -\frac{\mathrm{J}^z S^2(N-1)}{2} & \text{if } \mathrm{J}^z S > t + \frac{\Delta}{N-1}, \\ -\frac{S(N-1)t}{2} - \frac{S\Delta}{2} & \text{if } \mathrm{J}^z S < t + \frac{\Delta}{N-1}; \end{cases} \tag{19a}$$

$$E_{0,OBC}^{odd} = \begin{cases} -\frac{\mathrm{J}^z S^2(N-1)}{2} & \text{if } \mathrm{J}^z S > t, \\ -\frac{S(N-1)t}{2} & \text{if } \mathrm{J}^z S < t; \end{cases} \tag{19b}$$

$$E_{0,PBC} = \begin{cases} -\frac{\mathrm{J}^z S^2 N}{2} & \text{if } \mathrm{J}^z S > t, \\ -\frac{NSt}{2} & \text{if } \mathrm{J}^z S < t. \end{cases} \tag{19c}$$

Hence, the ordering of the GS depends on the relative magnitude of the exchange interaction with respect to the aniotropic interactions. In the regime where the anisotropic exchange dominates, the lowest energy configuration corresponds to a periodic non collinear alignment of spins in the xy plane, see Figure 3. This is a consequence of the DMI, the energy of which is minimized when $\hat{\vec{S}}_i$ and $\hat{\vec{S}}_j$ – where we consider $i = j \pm 1$ – lie in the plane perpendicular to the DMI vector $\vec{D}$ given in Eq. (7b) and

are perpendicular to one another. In contrast, when the isotropic exchange dominates, the GS is the ferromagnetic (FM) state where all the spins are pointing in the z-direction as shown in Figure 4. Thus the system exhibits a first order phase transition as shown in Figure 2.

Moreover, we note that in the regime where the anisotropic exchange dominates, both spiral states (i.e. Figure 3) are degenerate in energy in the case of the chain with PBC and the chain with OBC and an odd number of sites. This is not the case for the chain with OBC and an even number of sites, where the state defined by $\varphi_j^{(2)}$, see Figure 3b has a higher energy than the one defined by $\varphi_j^{(1)}$, see Figure 3a.

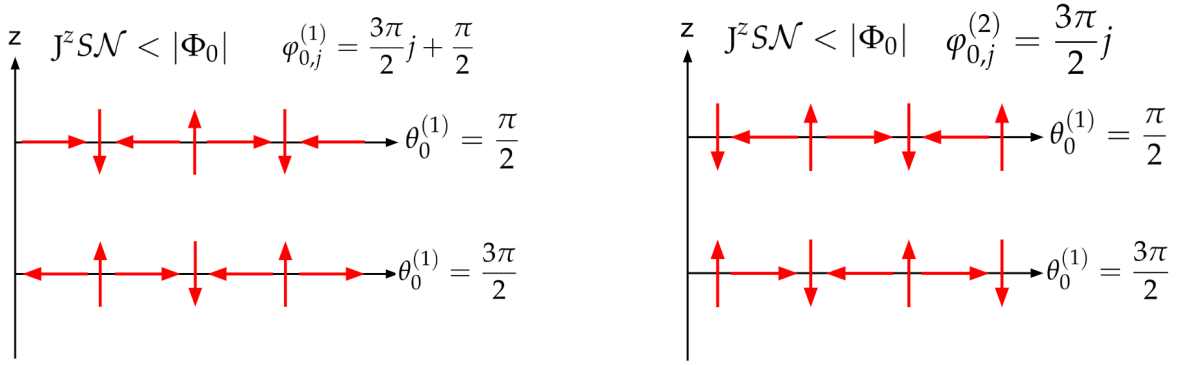

(a) (b)

Figure 3: GS of the chain for $B = 0$ in the regime where the anisotropic exchange dominates. The spins are situated in the xy plane forming a periodic spiral pattern with a period of four spins. The two states are related by a phase of $\pi/2$ in the definition of the azimuthal angle leading to a translation of one site. **(a)** GS of the chain with OBC for any number of sites and PBC. **(b)** GS of the chain with OBC and an odd number of sites and PBC.

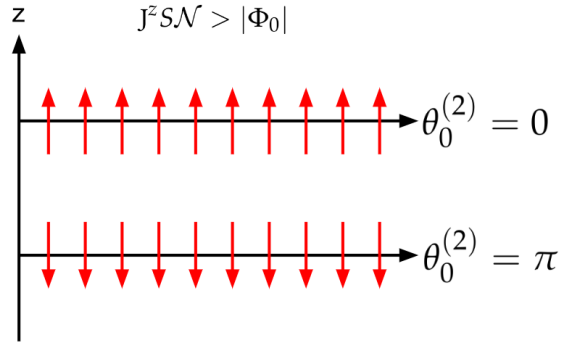

Figure 4: GS of the chain for $B = 0$ in the regime where the isotropic exchange dominates. Ferromagnetic alignment of the spins in the z-direction.

3.2 Ground state in an applied magnetic field

When a non-zero magnetic field parallel to the z-axis is added to the system, the lowest energy configuration is given by $\theta = n\pi$, where n is an integer whose sign depends on the direction of the magnetic field and the relative magnitude between the exchange interactions. Eq. (16b) leads to the condition

$$(-1)^{n+s_B} N|B| > |\Phi_0| - J^z S\mathcal{N}, \tag{20}$$

where we defined

$$s_B = \begin{cases} 0 & \text{if } B > 0, \\ 1 & \text{if } B < 0. \end{cases} \tag{21}$$

When the isotropic exchange dominates, Eq. (20) is satisfied when $n + s_B$ even, i.e. the spins are parallel to the magnetic field, and when $n + s_B$ is odd and $J^z S\mathcal{N} - N|B| > |\Phi_0|$. Hence, even if the magnetic field is antiparallel to the spin, the state is stable as long as the magnitude of the field is small enough, however this situation has a higher energy than the one where the field is parallel to the spins.
When the anisotropic exchange dominates, we require both the spins to be parallel to the magnetic field (i.e. $n + s_B$ even) and $J^z S\mathcal{N} + N|B| > |\Phi_0|$. This means that for the system to be stable, the magnetic field must be strong enough to overcome the anisotropic exchange's tendency to put the spins in the xy plane. Therefore, the system no longer exhibits a phase transition in the presence of a magnetic field.

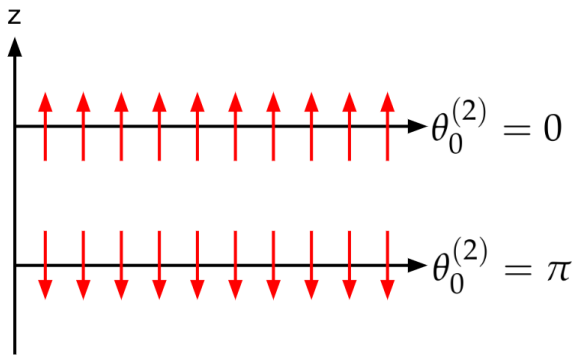

Figure 5: Ground state of the model when a magnetic field in the z direction is applied. The GS is unique and given by the ferromagnetic alignment of the spins with a direction determined by the direction of the magnetic field and the relative magnitude of the exchange interactions.

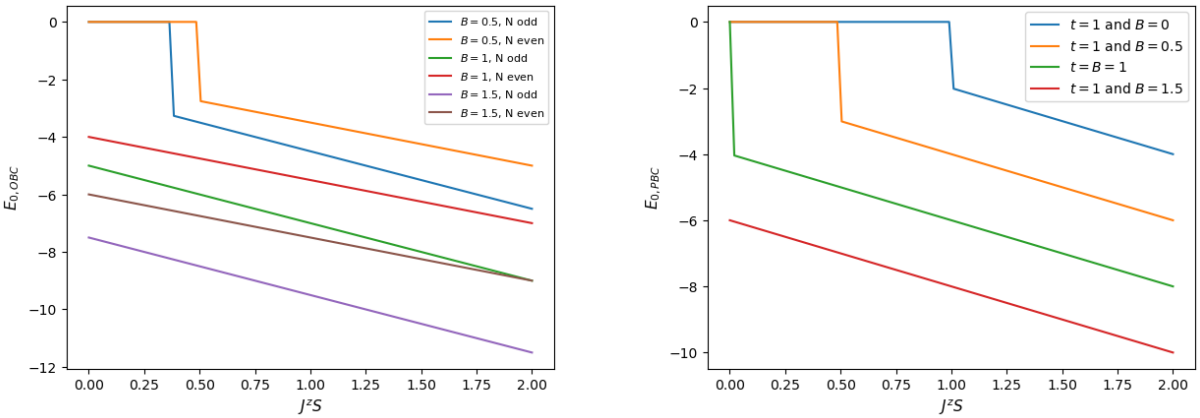

(a) (b)

Figure 6: Ground state energy of the chain as a function of the isotropic exchange parameter $J^z S$ for $t = 1$, $\Delta = 0.5$ and different values of the magnetic field B. **(a)** Ground state energy for the chain with OBC in the case of an even number of sites ($N = 4$) and an odd number of sites ($N = 5$). **(b)** Ground state energy for the chain with PBC and $N = 4$.

The GS corresponds to the FM state illustrated in Figure 5 and has energy

$$E_{0,OBC}^{even} = -\frac{J^z S^2 (N-1)}{2} - BSN \quad \text{if} \quad J^z S(N-1) + BN > (N-1)t + \Delta, \tag{22a}$$

$$E_{0,OBC}^{odd} = -\frac{J^z S^2 (N-1)}{2} - BSN \quad \text{if} \quad J^z S(N-1) + BN > (N-1)t, \tag{22b}$$

$$E_{0,PBC} - \frac{J^z S^2 N}{2} - BSN \quad \text{if} \quad J^z S + B > t. \tag{22c}$$

Figure 6 shows the ground state energy as a function of the isotropic exchange parameter $J^z S$, and

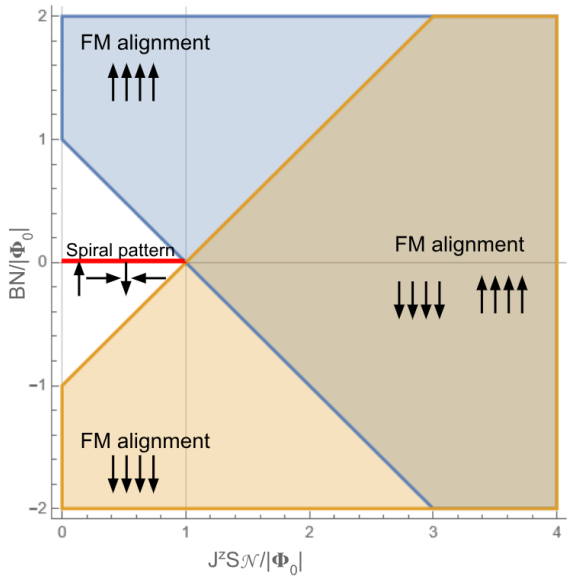

Figure 7: Phase diagram in the $(J^z S/|\Phi_0|, B/|\Phi_0|)$ plane with Φ_0 the value of the anisotropic exchange given in Eq. (15). For $B = 0$, there are two possible GS: the non-collinear ground state (red) and the FM state (blue and orange). When $B \neq 0$, the GS corresponds to the FM state; the direction of the spins depends on the value of the magnetic field. The blue region corresponds to the FM alignment in the $+z$ direction and the orange region to the alignment in the $-z$ direction. We also see that there is a region in which both FM alignments are stable. The white area indicates the regime in which the system is unstable.

represents that for a given value of the exchange parameters, a higher value of the magnetic field B lowers the energy of the system.

We have seen in Section 3.1 that when no magnetic field is applied, the system exhibits a phase transition with respect to $J^z S$. Figure 7 shows that in the regime where the anisotropic exchange dominates, the model also exhibits a phase transition with respect to the magnetic field (B). When $B = 0$, the system is in the non-collinear state illustrated in Figure 3. Once the magnetic field is added, the system becomes unstable[4] until $J^z S\mathcal{N} + NB > |\Phi_0|$ in which case the system is in the FM state shown in Figure 6.
Having found the ground states of the model, we now look at the dynamics of the excitations in the chain. To do so, we use a linearized Holstein-Primakhoff transformation.

4 Holstein-Primakhoff transformation

The Holstein-Primakhoff transformation (HPT) is a map between the bosonic creation and annihilation operators ($\hat{a}^\dagger$, $\hat{a}$) and the spin operators ($\hat{\vec{S}}$). It was first introduced in 1940 by T. Holstein and H. Primakhoff [18] in order to study spin waves in ferromagnets. The HPT relies on the fact that the spin ladder operators act on spin states in a similar way as the bosonic creation and annihilation operators do in Fock space.
In this mapping, we consider that the vacuum has spin $+S$ in the direction $\vec{\Omega}_j$ of the GS, and each HP boson represents a perturbation from the classical GS.

[4]The white region in Figure 7 corresponds to a regime where the Hamiltonian cannot be minimized: The first derivative vanishes for $\theta = n\pi$, however the second derivative is negative, which corresponds to a state of maxima energy.

By defining the rotated local coordinate system

$$\begin{pmatrix} \hat{e}_j^{(1)} \\ \hat{e}_j^{(2)} \\ \hat{e}_j^{(3)} \end{pmatrix} = \begin{pmatrix} \cos\theta\cos\varphi_j & \cos\theta\sin\varphi_j & -\sin\theta \\ -\sin\varphi_j & \cos\varphi_j & 0 \\ \sin\theta\cos\varphi_j & \sin\theta\sin\varphi_j & \cos\theta \end{pmatrix} \begin{pmatrix} \hat{x} \\ \hat{y} \\ \hat{z} \end{pmatrix} \tag{23}$$

with $\hat{e}_j^{(3)} = \vec{\Omega}_j$ the direction of the GS, the generic HPT is given by [19]

$$\hat{\vec{S}}_j \cdot \vec{\Omega}_j = S - \hat{a}_j^\dagger \hat{a}_j, \tag{24a}$$

$$\hat{S}_j^+ = \hat{\vec{S}}_j \cdot \hat{e}_j^{(1)} + i\hat{\vec{S}}_j \cdot \hat{e}_j^{(2)} = \sqrt{2S - \hat{a}_j^\dagger \hat{a}_j}\hat{a}_j, \tag{24b}$$

$$\hat{S}_j^- = \hat{\vec{S}}_j \cdot \hat{e}_j^{(1)} - i\hat{\vec{S}}_j \cdot \hat{e}_j^{(2)} = \hat{a}_j^\dagger \sqrt{2S - \hat{a}_j^\dagger \hat{a}_j}, \tag{24c}$$

where the prefactor $\sqrt{2S - \hat{a}_j^\dagger \hat{a}_j}$ in the definition of the spin ladder operators ensures that the maximum number of spins in a given site is $2S$.

Since we are interested in studying the behaviour of the system near its GS, we take a linear approximation, where we only allow for small perturbations around the GS by assuming that $\langle \hat{a}_j^\dagger \hat{a}_j \rangle \ll S$. By expanding the prefactor to its lowest order we obtain $\sqrt{2S - \hat{a}_j^\dagger \hat{a}_j} \simeq \sqrt{2S} + ...$, thus the linear Holstein-Primakhoff transformation (LHPT) reads

$$\hat{\vec{S}}_j \cdot \vec{\Omega}_j = S - \hat{a}_j^\dagger \hat{a}_j, \tag{25a}$$

$$\hat{S}_j^+ = \hat{\vec{S}}_j \cdot \hat{e}_j^{(1)} + i\hat{\vec{S}}_j \cdot \hat{e}_j^{(2)} \simeq \sqrt{2S}\hat{a}_j, \tag{25b}$$

$$\hat{S}_j^- = \hat{\vec{S}}_j \cdot \hat{e}_j^{(1)} - i\hat{\vec{S}}_j \cdot \hat{e}_j^{(2)} \simeq \sqrt{2S}\hat{a}_j^\dagger. \tag{25c}$$

4.1 Linearisation around the ferromagnetic state: The BKC

In the regime where the isotropic exchange dominates, i.e. $\mathrm{J}^z S\mathcal{N} + N|B| > |\Phi_0|$, the GS of the system is given by the FM state. This is the state defined by $\theta = n\pi$ ($n \in \mathbb{Z}$) where all the spins are pointing in the z-direction. Without loss of generality we can chose $n = 0$, that is $\vec{\Omega}_j = \hat{z}$ to obtain the usual LHPT

$$\hat{S}_j^z = S - \hat{a}_j^\dagger \hat{a}_j, \tag{26a}$$

$$\hat{S}_j^+ = \hat{S}_j^x + i\hat{S}_j^y \simeq \sqrt{2S}\hat{a}_j, \tag{26b}$$

$$\hat{S}_j^- = \hat{S}_j^x - i\hat{S}_j^y \simeq \sqrt{2S}\hat{a}_j^\dagger, \tag{26c}$$

which can be rearranged to yield

$$\hat{S}_j^x \simeq \sqrt{2S}\hat{x}_j, \tag{27a}$$

$$\hat{S}_j^y \simeq \sqrt{2S}\hat{p}_j. \tag{27b}$$

Thus for the magnonic BKC, the x and y components of the spin act as the $\hat{x}$ and $\hat{p}$ quadratures respectively. Moreover, we remark that due to the linear approximation the algebra of the spin operators is no longer that of the Lie group but is now given by

$$[\hat{S}_j^+, \hat{S}_{j'}^-] = 2S\delta_{j,j'} \tag{28a}$$

$$[\hat{S}_j^z, \hat{S}_{j'}^\pm] = \pm\hat{S}_j^\pm \delta_{j,j'} \tag{28b}$$

$$[\hat{S}^x_j, \hat{S}^y_{j'}] = iS\delta_{j,j'} \tag{28c}$$

$$[\hat{S}^z_j, \hat{S}^x_{j'}] = i\hat{S}^y_j\delta_{j,j'} \tag{28d}$$

$$[\hat{S}^y_j, \hat{S}^z_{j'}] = i\hat{S}^x_j\delta_{j,j'} \tag{28e}$$

instead (see Appendix A for derivation). By applying the LHPT Eq. (27) to the spin Hamiltonian Eq. (6), we obtain the linearized Hamiltonian

$$\begin{aligned}\hat{H} = &\frac{1}{2}\sum_j \left(it(\hat{a}^\dagger_{j+1}\hat{a}_j - \hat{a}^\dagger_j\hat{a}_{j+1}) + i\Delta(\hat{a}^\dagger_{j+1}\hat{a}^\dagger_j - \hat{a}_j\hat{a}_{j+1})\right) + \frac{J^zS}{2}\sum_j(\hat{a}^\dagger_j\hat{a}_j + \hat{a}^\dagger_{j+1}\hat{a}_{j+1}) \\ &+ B\sum_j \hat{a}^\dagger_j\hat{a}_j - \frac{J^zS^2\mathcal{N}}{2} - BSN,\end{aligned} \tag{29a}$$

$$\begin{aligned}\hat{H} = &\frac{1}{2}\sum_j \left(-(t-\Delta)\hat{x}_{j+1}\hat{p}_j + (t+\Delta)\hat{p}_{j+1}\hat{x}_j\right) + \frac{J^zS}{4}\sum_j(\hat{x}^2_j + \hat{p}^2_j + \hat{x}^2_{j+1} + \hat{p}^2_{j+1}) \\ &+ \frac{B}{2}\sum_j(\hat{x}^2_j + \hat{p}^2_j) - J^zS^2\mathcal{N} - 2BSN,\end{aligned} \tag{29b}$$

where we used Eq. (3) to obtain the Hamiltonian in terms of the quadratures.
We see that this Hamiltonian contains two parts; the first part, which arises from the anisotropic exchange, corresponds to the Hamiltonian of the BKC Eq. (1). The second part, which arises from both the isotropic exchange and the magnetic field, contains a constant term and a part proportional to the number operator. Figure 8 shows that this additional term, which arises from the addition of the isotropic exchange and the magnetic field, breaks the asymmetry in the coupling between $\hat{x}_j$ and $\hat{p}_{j\pm1}$ and couples the quadratures to themselves, leading to different dynamics which we study in Section 5.
Hence, we have managed the goal of the thesis; in the regime where the isotropic exchange dominates

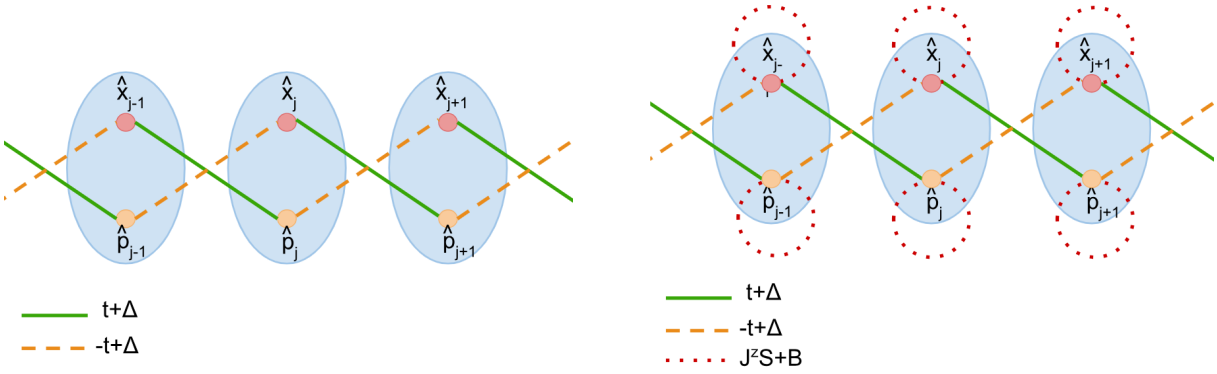

(a) (b)

Figure 8: Schematic representation of the coupling between quadratures in the BKC. **(a)** Coupling between quadratures in the photonic BKC. **(b)** Coupling between quadratures in the magnonic BKC. In the magnonic case (b), the quadratures couple to themselves, breaking the asymmetry of the photonic case (a).

and the spins are aligned in the FM state, Eq. (6) defines the magnonic BKC.

4.2 Linearisation around the non collinear state

We now linearise the Hamiltonian around the non-collinear states Figure 3, for which we consider the Hamiltonian Eq. (6) with no magnetic field, i.e. $B = 0$, in the regime where the anisotropic exchange dominates, that is $|\Phi_0| > J^zS\mathcal{N}$. This GS is characterized by both the polar and azimuthal angles and

are related by a $\pi/2$ phase in the azimuthal angle ($\varphi_{0,j}^{(1)} = \varphi_{0,j}^{(2)} + \pi/2$) or by a translation of one site. Since the Hamiltonian has a period equal to π, the two GS lead to different Hamiltonians[5]. Moreover, since the choice of the integers n and n_j is only restricted to the condition $n_j + n_{j\pm1}$ odd, we can set $n = 0$ and $n_j = j$ without loss of generality.

4.2.1 Linearisation around the spin spiral state 1

The GS of the spin spiral state 1 is defined by $\varphi_{0,j}^{(1)} = \frac{3\pi}{2}j + \frac{\pi}{2}$ and $\theta_0^{(1)} = \frac{\pi}{2}$ hence the GS vector is $\vec{\Omega}_j = -\sin\frac{3\pi}{2}j \cdot \hat{x} + \cos\frac{3\pi}{2}j \cdot \hat{y}$. We introduce it into Eq. (24) to obtain the LHPT

$$-\hat{S}_j^x \sin\frac{3\pi}{2}j + \hat{S}_j^y \cos\frac{3\pi}{2}j = S - \hat{a}_j^\dagger \hat{a}_j, \tag{30a}$$

$$-i\hat{S}_j^x \cos\frac{3\pi}{2}j - i\hat{S}_j^y \sin\frac{3\pi}{2}j - \hat{S}_j^z \simeq \sqrt{2S}\hat{a}_j, \tag{30b}$$

$$i\hat{S}_j^x \cos\frac{3\pi}{2}j + i\hat{S}_j^y \sin\frac{3\pi}{2}j - \hat{S}_j^z \simeq \sqrt{2S}\hat{a}_j^\dagger. \tag{30c}$$

We now rearrange it as

$$\begin{aligned}\hat{S}_j^x &\simeq -(S - \hat{a}_j^\dagger \hat{a}_j)\sin\frac{3\pi}{2}j + \frac{\sqrt{2S}}{2i}(\hat{a}_j^\dagger - \hat{a}_j)\cos\frac{3\pi}{2}j; \\ &= -(S - \hat{a}_j^\dagger \hat{a}_j)\sin\frac{3\pi}{2}j + \sqrt{2S}\hat{p}_j \cos\frac{3\pi}{2}j,\end{aligned} \tag{31a}$$

$$\begin{aligned}\hat{S}_j^y &\simeq (S - \hat{a}_j^\dagger \hat{a}_j)\cos\frac{3\pi}{2}j + \frac{\sqrt{2S}}{2i}(\hat{a}_j^\dagger - \hat{a}_j)\sin\frac{3\pi}{2}j; \\ &= (S - \hat{a}_j^\dagger \hat{a}_j)\cos\frac{3\pi}{2}j + \sqrt{2S}\hat{p}_j \sin\frac{3\pi}{2}j,\end{aligned} \tag{31b}$$

$$\begin{aligned}\hat{S}_j^z &\simeq -\frac{\sqrt{2S}}{2}(\hat{a}_j^\dagger + \hat{a}_j); \\ &= -\sqrt{2S}\hat{x}_j,\end{aligned} \tag{31c}$$

where the algebra of the spin operators is now given by

$$[\hat{S}_j^x, \hat{S}_{j'}^y] = i\hat{S}_j^z \delta_{j,j'}, \tag{32a}$$

$$[\hat{S}_j^z, \hat{S}_{j'}^x] = i\left(S\cos\frac{3\pi}{2}j + \hat{S}^y \sin^2\frac{3\pi}{2}j\right)\delta_{j,j'}, \tag{32b}$$

$$[\hat{S}_j^y, \hat{S}_{j'}^z] = i\left(-S\sin\frac{3\pi}{2}j + \hat{S}^x \cos^2\frac{3\pi}{2}j\right)\delta_{j,j'}. \tag{32c}$$

We see that while the z component of the spin always maps to the x quadrature, both the x and y components of the spin act as the p quadrature. This is due to the non-collinear nature of the GS (see Figure 3a) and the fact that the excitations propagate in the plane perpendicular to the ground state, as we further explain in Section 6.1. At odd sites, the spins of the GS are in the x direction, hence it is the y component of the spin $\hat{S}^y$ that acts as the p-quadrature. Then, at even sites, the spins of the GS are in

[5]A phase π corresponds to a translation by two spins, which may sound wrong since the pattern obviously contains fours spins. However, as for the FM case with no magnetic field added, where the state with all spins pointing up and the one with all spins pointing down are virtually the same, when there are no further constrictions (such as a magnetic field in the x or y direction), the states related by a translation of two spins are basically the same.

the y direction, meaning that the x component of the spin corresponds to the p quadrature. By plugging Eq. (31) into the Hamiltonian Eq. (6) we obtain

$$\hat{H}_1 = \frac{1}{2}\sum_j \left(-(t-(-1)^j\Delta)(S-(\hat{n}_{j+1}+\hat{n}_j)) + \frac{1}{2}(t+(-1)^j\Delta)(\hat{a}_{j+1}^\dagger - \hat{a}_{j+1})(\hat{a}_j^\dagger - \hat{a}_j) \right) - \frac{J^z S}{4}\sum_j (\hat{a}_{j+1}^\dagger + \hat{a}_{j+1})(\hat{a}_j^\dagger + \hat{a}_j); \tag{33a}$$

$$\hat{H}_1^{OBC} = \frac{-(S+1)}{2}\sum_j (t-(-1)^j\Delta) + \frac{1}{4}((t+\Delta)(\hat{x}_1^2+\hat{p}_1^2) + (t-(-1)^N\Delta)(\hat{x}_N^2+\hat{p}_N^2)) + \frac{1}{2}\sum_{j=2}^{N-1}\left(t(\hat{x}_j^2+\hat{p}_j^2) - (t+(-1)^j\Delta)\hat{p}_{j+1}\hat{p}_j - J^z S\,\hat{x}_{j+1}\hat{x}_j \right); \tag{33b}$$

$$\hat{H}_1^{PBC} = \frac{-N(S+1)t}{2} + \frac{1}{2}\sum_{j=1}^{N}\left(t(\hat{x}_j^2+\hat{p}_j^2) - (t+(-1)^j\Delta)\hat{p}_{j+1}\hat{p}_j - J^z S\,\hat{x}_{j+1}\hat{x}_j \right), \tag{33c}$$

where we have used Eq. (3) to write the Hamiltonian in terms of quadratures.

Figure 9b shows the coupling of the quadratures in the chain, where the blue circles represent the odd sites (the sites where $\hat{S}^y$ acts as the p quadrature) and the pink circles correspond to the even sites (where $\hat{S}^x$ acts as the p quadrature). We note that contrary to the photonic BKC, where the quadratures only couple to each other, in this case, the quadratures only couple to themselves, either at a neighbouring site or at the same site.

4.2.2 Linearisation around the spin spiral state 2

The GS is now defined by $\varphi_{0,j}^{(2)} = \frac{3\pi}{2}j$ and $\theta_0^{(1)} = \frac{\pi}{2}$ hence the GS vector is $\vec{\Omega}_j = \cos\frac{3\pi}{2}j\cdot\hat{x} + \sin\frac{3\pi}{2}j\cdot\hat{y}$. We introduce it into Eq. (24) to obtain the LHPT

$$\hat{S}_j^x\cos\frac{3\pi}{2}j + \hat{S}_j^y\sin\frac{3\pi}{2}j = S - \hat{a}_j^\dagger\hat{a}_j, \tag{34a}$$

$$-i\hat{S}_j^x\sin\frac{3\pi}{2}j + i\hat{S}_j^y\cos\frac{3\pi}{2}j - \hat{S}_j^z \simeq \sqrt{2S}\hat{a}_j, \tag{34b}$$

$$i\hat{S}_j^x\sin\frac{3\pi}{2}j - i\hat{S}_j^y\cos\frac{3\pi}{2}j - \hat{S}_j^z \simeq \sqrt{2S}\hat{a}_j^\dagger, \tag{34c}$$

which can be rearranged as

$$\hat{S}_j^x \simeq (S-\hat{a}_j^\dagger\hat{a}_j)\cos\frac{3\pi}{2}j + \sqrt{2S}\hat{p}_j\sin\frac{3\pi}{2}j, \tag{35a}$$

$$\hat{S}_j^y \simeq (S-\hat{a}_j^\dagger\hat{a}_j)\sin\frac{3\pi}{2}j - \sqrt{2S}\hat{p}_j\cos\frac{3\pi}{2}j, \tag{35b}$$

$$\hat{S}_j^z \simeq -\sqrt{2S}\hat{x}_j. \tag{35c}$$

In this case the algebra of the spin operators is given by

$$[\hat{S}_j^x, \hat{S}_{j'}^y] = i\hat{S}_j^z\delta_{j,j'}, \tag{36a}$$

$$[\hat{S}_j^z, \hat{S}_{j'}^x] = i\left(S\sin\frac{3\pi}{2}j + \hat{S}^y\cos^2\frac{3\pi}{2}j\right)\delta_{j,j'}, \tag{36b}$$

$$[\hat{S}_j^y, \hat{S}_{j'}^z] = i\left(S\cos\frac{3\pi}{2}j + \hat{S}^x\sin^2\frac{3\pi}{2}j\right)\delta_{j,j'}. \tag{36c}$$

As for the spin spiral 1, the z component of the spin maps to the x quadrature, while the x and y component act as the p quadrature on alternating sites. However, we see in Figure 3b that in this case, it is the x component that acts as the p quadrature in odd sites and the y component in the even sites. This is to be expected since the two states are related by a phase $\pi/2$, corresponding to a translation by one site.
By plugging it into the Hamiltonian Eq. (6) we obtain

$$\hat{H}_2 = \frac{1}{2}\sum_j \left(-(t+(-1)^j\Delta)(S-(\hat{n}_{j+1}+\hat{n}_j)) + \frac{1}{2}(t-(-1)^j\Delta)(\hat{a}^\dagger_{j+1}-\hat{a}_{j+1})(\hat{a}^\dagger_j-\hat{a}_j)\right) - \frac{J^z S}{4}\sum_j (\hat{a}^\dagger_{j+1}+\hat{a}_{j+1})(\hat{a}^\dagger_j+\hat{a}_j), \tag{37a}$$

$$= C + \frac{1}{2}\sum_j \left(\frac{(t+(-1)^j\Delta)}{2}(\hat{x}^2_{j+1}+\hat{p}^2_{j+1}+\hat{x}^2_j+\hat{p}^2_j) - (t-(-1)^j\Delta)\hat{p}_{j+1}\hat{p}_j - J^z S\,\hat{x}_{j+1}\hat{x}_j\right), \tag{37b}$$

with $C := -(S+1)/2\sum_j(t+(-1)^j\Delta)$ a constant that depends on the number of sites and boundary conditions.
As illustrated in Figure 9b, where the pink and blue circles now correspond to the odd sites and the even sites, respectively, the quadratures only couple to themselves. We remark that in the case of OBC

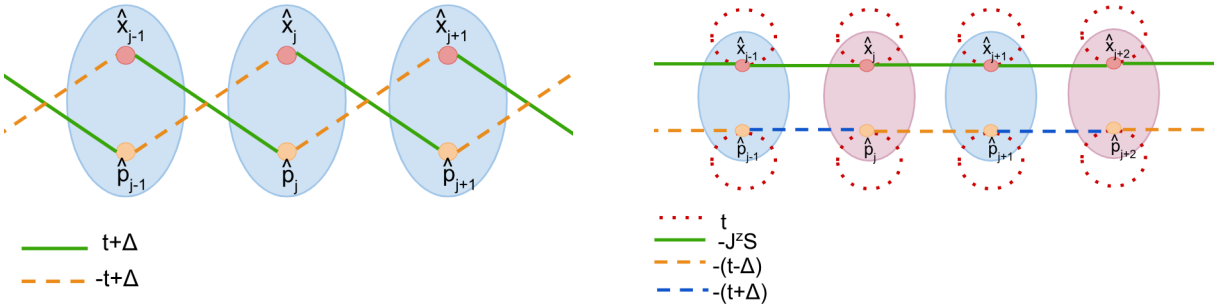

(a) (b)

Figure 9: Schematic representation of the coupling between quadratures. **(a)** Coupling between quadratures in the photonic BKC. The quadratures only couple to each other in a spatially asymmetric manner [16]. **(b)** Coupling between quadratures in the spin spiral chain for PBC and the bulk part of the chain with OBC. For the spiral chain 1 (defined in Section 4.2.1), the blue sites correspond to j odd and the pink sites correspond to j even. The opposite is true for the spiral chain 2 (defined in Section 4.2.2); the blue sites correspond to j even and the pink sites to j odd.

the coupling between the x quadratures at neighbouring sites is uniform at the bulk of the chain but is different for the first and last spin due to the lack of one of their neighbours.

5 Properties of the spin implementation of the bosonic Kitaev chain

We now focus on the spin version of the BKC described by Eq. (29) to see how it differs from the photonic BKC Eq. (1) [16]. Throughout this section, we consider the regime where $J^z S\mathcal{N} + NB > |\Phi_0|$ to ensure the stability of the ground state.

5.1 Winding number

As the photonic BKC, the magnonic BKC has a non-trivial topology with a winding number of one. This can be seen by Fourier transforming Eq. (29) to write it in the momentum space as

$$\hat{H} = \frac{1}{2}\sum_{k\in 1\mathrm{BZ}} \hat{\vec{A}}_k^\dagger [\vec{h}_B(k)\cdot\hat{\vec{\sigma}}]\hat{\vec{A}}_k + \frac{1}{2}\sum_{k\in 1\mathrm{BZ}} \hat{\vec{A}}_k^\dagger [(\mathrm{J}^z S + B)\cdot \mathbb{1}_2]\hat{\vec{A}}_k - \frac{\mathrm{J}^z S^2 \mathcal{N}}{2} - BSN,$$

where $\mathbb{1}_2$ is the 2×2 identity matrix and the first term corresponds to Eq. (2). By defining the Pauli 4-vector $\underline{\sigma} = (\mathbb{1}_2, \hat{\vec{\sigma}})$ and $\underline{h}(k) = (\mathrm{J}^z S + B, \vec{h}_B(k))$, the Hamiltonian reads

$$\hat{H} = \frac{1}{2}\sum_{k\in 1\mathrm{BZ}} \hat{\vec{A}}_k^\dagger [\underline{h}(k)\cdot\underline{\sigma}]\hat{\vec{A}}_k - \frac{\mathrm{J}^z S^2 \mathcal{N}}{2} - BSN. \tag{38}$$

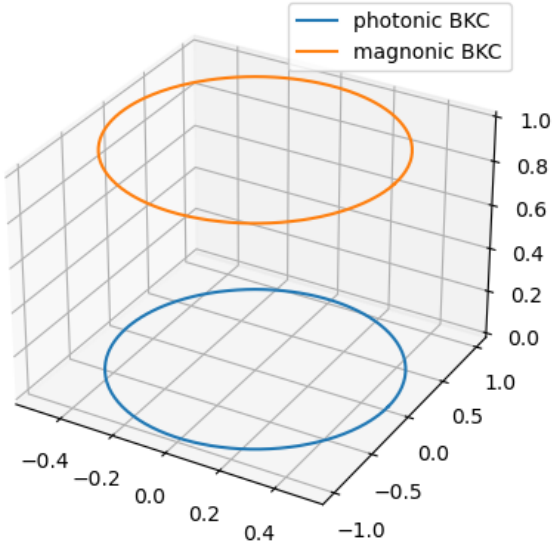

Figure 10: $\underline{h}(k)$ and $\vec{h}_B(k)$ for $t = \mathrm{J}^z S + B = 1$ and $\Delta = 0.5$. The isotropic exchange and magnetic field shift the vector $\vec{h}_B(k)$ to $\underline{h}(k)$ which winds once around the origin.

Figure 10 shows that the term proportional to the identity which arises from the isotropic exchange and the magnetic field corresponds to a shift in the vector $\vec{h}_B$ while leaving the winding number unchanged.
To see the consequences of the non-trivial topology of the model, we now examine the dynamics of the excitations in the chain by looking at the equations of motion.

5.2 Equations of motion

To study the dynamics of a spin wave excitation in the chain, we start by considering that the system is in the FM state with all the spins pointing in the positive z-direction[6] and allowing for small fluctuations $\delta\hat{\vec{S}}_j = (\delta\hat{S}_j^x, \delta\hat{S}_j^y, S)$ – with $\delta S^{\hat{x}/y}{}_j \ll S$– around the GS. The linearised Heisenberg equations of motion are given by

$$\delta\dot{\hat{S}}_j^x = \frac{t+\Delta}{2}\delta\hat{S}_{j-1}^x - \frac{t-\Delta}{2}\delta\hat{S}_{j+1}^x + (\mathrm{J}^z S + B)\delta\hat{S}_j^y, \tag{39a}$$

$$\delta\dot{\hat{S}}_j^y = \frac{t-\Delta}{2}\delta\hat{S}_{j-1}^y - \frac{t+\Delta}{2}\delta\hat{S}_{j+1}^y - (\mathrm{J}^z S + B)\delta\hat{S}_j^x, \tag{39b}$$

[6]This is fair to assume since the result would be the same if we were to consider the state where all the spins are pointing to the negative z-direction.

$$\dot{\hat{S}}_j^z = 0, \tag{39c}$$

where we used the algebra defined in Eq. (28). Equivalently, the equations of motion in terms of the spin ladder operators read

$$\delta\dot{\hat{S}}_j^+ = -\frac{t}{2}(\delta\hat{S}_{j+1}^+ - \delta\hat{S}_{j-1}^+) + \frac{\Delta}{2}(\delta\hat{S}_{j+1}^- + \delta\hat{S}_{j-1}^-) - i(\mathrm{J}^z S + B)\delta\hat{S}_j^+, \tag{40a}$$

$$\delta\dot{\hat{S}}_j^- = -\frac{t}{2}(\delta\hat{S}_{j+1}^- - \delta\hat{S}_{j-1}^-) + \frac{\Delta}{2}(\delta\hat{S}_{j+1}^+ + \delta\hat{S}_{j-1}^+) + i(\mathrm{J}^z S + B)\delta\hat{S}_j^-. \tag{40b}$$

We note that the first two terms of Eq. (39) show a remarkable similarity to the equations of motion of the BKC Eq. (5); for $\mathrm{J}^z S + B = 0$, we have the directional transport of magnons with a direction depending on the phase of the excitation. In this limit, the x and y components of the spin are forced by its neighbours in a spatially asymmetric way; if we focus on Eq. (39a) (Eq. (39b) respectively), we see that there is an increase in amplitude as the wave propagates from left to right (right to left), and a decrease in amplitude when it propagates in the opposite direction. This means that the spin wave is amplified in one direction and deamplified in the opposite one.

This asymmetry is broken when $\mathrm{J}^z S + B \neq 0$; the x and y components are no longer dynamically decoupled; as the excitation propagates through the chain, the isotropic exchange and magnetic field change the phase of the spin wave. In the case where an x-excitation is propagating in the chain, the first two terms of Eq. (39a) cause the excitation to be amplified as it propagates from left to right and to be deamplified as it propagates from right to left, respectively. The last term however changes the phase of the excitation, turning part of the x-excitation into a y-excitation. In turn, Eq. (39b) shows that the y-excitation exhibits the opposite behaviour; it is amplified when it propagates from the right to the left and deamplified from the left to the right. As before, the phase of the y-excitation then changes as a consequence of the isotropic exchange and the magnetic field.

The Heisenberg equations of motion corresponding to Eq. (29) are given by

$$\dot{\hat{x}}_j = \frac{t+\Delta}{2}\hat{x}_{j-1} - \frac{t-\Delta}{2}\hat{x}_{j+1} + (\mathrm{J}^z S + B)\hat{p}_j, \tag{41a}$$

$$\dot{\hat{p}}_j = \frac{t-\Delta}{2}\hat{p}_{j-1} - \frac{t+\Delta}{2}\hat{p}_{j+1} - (\mathrm{J}^z S + B)\hat{x}_j. \tag{41b}$$

They exhibit the same structure as Eq. (39). This is in accordance with the LHPT Eq. (27), which shows that the x and y components of the spin in the magnonic BKC take the role of the quadratures in the photonic BKC. Therefore, by adding a term of the form $E\sum_j \hat{a}_j^\dagger \hat{a}_j$ to the photonic BKC, the quadratures are no longer dynamically decoupled.
Consequently, the regime of stability of the magnonic BKC is different to that of the photonic BKC. In order to see these changes, we now compute the dispersion relation of the system in the case of PBC and OBC.

5.3 Dispersion relation

5.3.1 Periodic boundary conditions

In the case of PBC, the Hamiltonian is diagonal in the basis of plane waves

$$\delta\hat{S}_j^{x,y} = A_{x,y}e^{i(kj-\omega\tau)}, \tag{42}$$

where $A_{x,y}$ is the amplitude of the wave, k denotes the wave vector, ω is the dispersion, and τ indicates the time. By plugging it into Eq. (39), we obtain the matrix equation $M(\omega)\cdot A = 0$, i.e.

$$\begin{pmatrix} (\Delta\cos(k) - it\sin(k)) + i\omega & \mathrm{J}^z S + B \\ -(\mathrm{J}^z S + B) & -(\Delta\cos(k) + it\sin(k)) + i\omega \end{pmatrix}\begin{pmatrix} A_x \\ A_y \end{pmatrix} = \begin{pmatrix} 0 \\ 0 \end{pmatrix}, \tag{43}$$

where $M(\omega)$ is the dynamical matrix of the system. The dispersion relation is then obtained by solving $\det(M(\omega)) = 0$, which yields

$$\omega_{\pm}(k) = t \sin k \pm \sqrt{(J^z S + B)^2 - \Delta^2 \cos^2 k}. \tag{44}$$

We can easily see that the dispersion is real for any value of the wave vector k as long as $J^z S + B \geq \Delta$. Since we are in the regime where $J^z S + B > t$, the system with PBC is always dynamically stable when $t > \Delta$. This is in contrast with the photonic BKC, where the system is always dynamically unstable due to the decoupling of the quadratures. Since the dynamics of the x and y components are independent of one another in the photonic BKC, an x- (y-) excitation is amplified as it propagates from left to right (right to left). In the case of PBC, the excitation would be able to keep propagating in a given direction , which would lead to an indefinite amplification. This is unphysical and would lead to instabilities in the system.

In the case of the magnonic BKC, when an x- (y-) excitation propagates from left to right (right to left), the amplification resulting from the symmetric anisotropic exchange is damped by the isotropic exchange and the magnetic field, coupling the two components. Thus. the system is dynamically stable since there is no amplification.

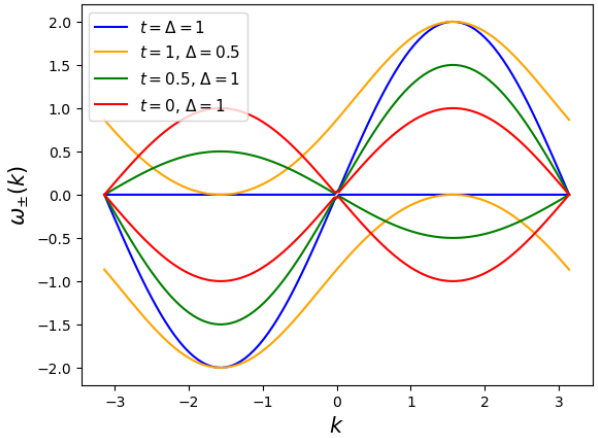

Figure 11: Dispersion relation of the magnonic BKC with PBC for $J^z S + B = 1$ and different values of the hopping parameter and the driving amplitude.

Figure 11 shows the dispersion relation of the system Eq. (44) in the regime where $t \geq \Delta$. In it we see that the system has two bands which touch in the limit where $J^z S + B = \Delta$ forming the characteristic shape of the Weyl cone at the center and edeges of the first Brillouin zone (i.e. at $k = 0$ and $k = \pm\pi$). These Weyl nodes, which arise from the broken mirror and time-reversal symmetries, correspond to a type-I node for the red and green curves ($t < 1$), and to a node at the horizon for the blue curve ($t = 1$) [20].
In order for the excitation to be amplified as it propagates through the chain, the driving amplitude must be large enough to overcome the damping, i.e. $\Delta > J^z S + B$. Eq. (22c) shows that the FM state is stable as long as the isotropic exchange and the magnetic field dominate over the DM interaction. By setting $\Delta > J^z S + B > t$, the magnonic BKC with PBC is well defined and allows for amplification. Figure 12 shows that the system is dynamically unstable in this regime; Eq. (44) has a non-zero imaginary part for $|\cos k| > (J^z S + B)/\Delta$. The origin of this instability is the same as that of the photonic BKC: the directional amplification of excitations together with the chiral nature of the chain lead to indefinite amplification in the case of PBC, causing the system to be unstable.

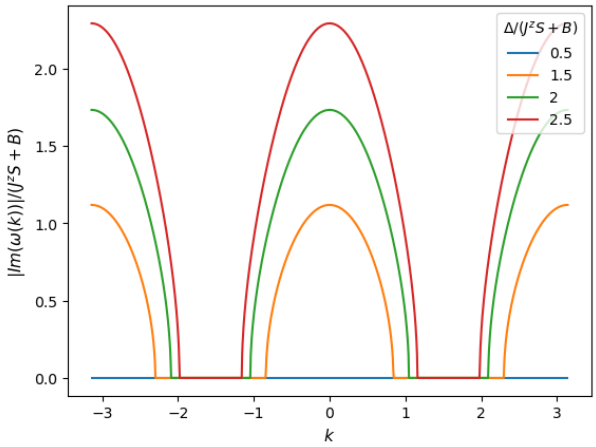

Figure 12: Imaginary part of the dispersion relation of the magnonic BKC as a function of the wavevector k for $J^zS + B = 1$, $t = 0.5(J^zS + B)$ and different values of the driving amplitude.

5.3.2 Open boundary conditions

When considering the system with open boundary conditions, the situation is remarkably different due to the presence of the edges of the chain. In the limit where $J^zS + B = 0$[7], the system is always dynamically stable for $t > \Delta$ since the finite size of the chain prevents for the excitations to be indefinetly amplified. This is not necessarily the case any longer when we add the isotropic exchange and magnetic field to the system. In reference [16] it is shown that the addition of on-site perturbations of the form $\omega_j \hat{a}_j^\dagger \hat{a}_j$ may cause instabilities even when $t > \Delta$ since such term changes the pase of the excitation. Due to the chirality of the chain, changing the phase of the excitation may lead to indefinite amplification, causing instabilities.
We will prove that contrary to the photonic case, due to the addition of the isotropic exchange and the magnetic field, the magnonic BKC can be stable even in the regime where $\Delta > t$ since these additional terms damp the amplification of the excitations.

In this section, we examine both situations and show that the model is diagonalized by a position dependent squeezing transformation (see Appendix B for derivation)

$$\hat{U}\hat{S}_j^+\hat{U}^\dagger = \hat{\tilde{S}}_j^+ \cosh(r(j-j_0)) + \hat{\tilde{S}}_j^- \sinh(r(j-j_0)), \tag{45a}$$

$$\hat{U}\hat{S}_j^-\hat{U}^\dagger = \hat{\tilde{S}}_j^+ \sinh(r(j-j_0)) + \hat{\tilde{S}}_j^- \cosh(r(j-j_0)), \tag{45b}$$

$$\hat{U}\hat{S}_j^z\hat{U}^\dagger = -\frac{1}{4S}(\hat{\tilde{S}}_j^+\hat{\tilde{S}}_j^- + \hat{\tilde{S}}_j^-\hat{\tilde{S}}_j^+)\cosh(2r(j-j_0)) - \frac{1}{4S}((\hat{\tilde{S}}_j^+)^2 + (\hat{\tilde{S}}_j^-)^2)\sinh(2r(j-j_0)), \tag{45c}$$

where j_0 is an arbitrary lattice site and r is the squeezing parameter the definition of which depends on the regime. Moreover, we look at the stability regime that arises from the addition of the Gilbert damping

$$\dot{\hat{\vec{S}}}_j\Big|_{GD} = \dot{\hat{\vec{S}}}_j - \alpha\hat{\vec{S}}_j \times \dot{\hat{\vec{S}}}_j \tag{46a}$$

$$\begin{aligned}\dot{\hat{S}}_j^+\Big|_{GD} &= \left(-\frac{t}{2}(\delta\hat{S}_{j+1}^+ - \delta\hat{S}_{j-1}^+) + \frac{\Delta}{2}(\delta\hat{S}_{j+1}^- + \delta\hat{S}_{j-1}^-) - i(J^zS+B)\delta\hat{S}_j^+\right)(1-i\alpha S),\\ &= (1-i\alpha S)\dot{\hat{S}}_j^+,\end{aligned} \tag{46b}$$

[7] This limit corresponds to the x and y components being dynamically decoupled.

$$\begin{aligned}\dot{\hat{S}}_j^-\Big|_{GD} &= \left(-\frac{t}{2}(\delta\hat{S}_{j+1}^- - \delta\hat{S}_{j-1}^-) + \frac{\Delta}{2}(\delta\hat{S}_{j+1}^+ + \delta\hat{S}_{j-1}^+) + i(\mathrm{J}^z S + B)\delta\hat{S}_j^-\right)(1 + i\alpha S), \\ &= (1 + i\alpha S)\dot{\hat{S}}_j^-,\end{aligned} \tag{46c}$$

where the dimensionless variable $\alpha > 0$ is the damping parameter. The addition of this term stabilizes the system, which goes to its ground state, and it will allow us to determine the regime of stability in each case.

$\mathbf{t > \Delta}$

In the regime where the hopping parameter is larger than the driving amplitude, the squeezing parameter r is defined by

$$e^{2r} = \frac{t + \Delta}{t - \Delta}. \tag{47}$$

By applying the squeezing transformation Eq. (45) together with the gauge transformation

$$\delta\hat{S}_j^{\pm} = e^{\pm i\pi j/2}\delta\hat{S}_j^{\pm} \tag{48}$$

to the linearised equations of motion Eq. (40), we obtain

$$\dot{\hat{\delta}}_j^+ = -\frac{i\tilde{t}}{2}(\delta\hat{\tilde{S}}_{j+1}^+ + \delta\hat{\tilde{S}}_{j-1}^+) - i(\mathrm{J}^z S + B)(\delta\hat{\tilde{S}}_j^+ \cosh(2r(j - j_0)) + (-1)^j\delta\hat{\tilde{S}}_j^- \sinh(2r(j - j_0))), \tag{49a}$$

$$\dot{\hat{\delta}}_j^- = \frac{i\tilde{t}}{2}(\delta\hat{\tilde{S}}_{j+1}^- + \delta\hat{\tilde{S}}_{j-1}^-) + i(\mathrm{J}^z S + B)(\delta\hat{\tilde{S}}_j^- \cosh(2r(j - j_0)) + (-1)^j\delta\hat{\tilde{S}}_j^+ \sinh(2r(j - j_0))). \tag{49b}$$

Since we consider the system with OBC, the eigenvectors are no longer given by plane waves but rather standing waves of the form

$$\delta\hat{\tilde{S}}_j^{\pm} = A_{\pm}e^{-i\omega\tau}\sin(k_n j), \tag{50}$$

where $k_n = n\pi/(N+1)$ is the wave vector and n is an integer. The equations of motion yield

$$\omega A_+ = (\tilde{t}\cos k_n + (\mathrm{J}^z S + B)\cosh(2r(j - j_0)))\,A_+ + (\mathrm{J}^z S + B)\sinh(2r(j - j_0))A_-, \tag{51a}$$

$$-\omega A_- = (\tilde{t}\cos k_n + (\mathrm{J}^z S + B)\cosh(2r(j - j_0)))\,A_- + (\mathrm{J}^z S + B)\sinh(2r(j - j_0))A_+. \tag{51b}$$

In order to write the matrix equation leading to the dispersion relation, we need to get rid of the j dependence that is left in the hyperbolic functions by requiring $r \ll 1$, that is $\Delta \ll t$. In particular, in Appendix C.1 we show that by chosing $\Delta = o(tN^{-\nu})$ with $\nu > 1$, the approximation holds even in the large N limit. By doing so we obtain

$$\omega A_+ = (\tilde{t}\cos k_n + (\mathrm{J}^z S + B))\,A_+, \tag{52a}$$

$$-\omega A_- = (\tilde{t}\cos k_n + (\mathrm{J}^z S + B))\,A_-, \tag{52b}$$

which can be rewritten in matrix form as

$$\begin{pmatrix} \tilde{t}\cos(k_n) + (\mathrm{J}^z S + B) - \omega & 0 \\ 0 & -\tilde{t}\cos(k_n) - (\mathrm{J}^z S + B) - \omega \end{pmatrix}\begin{pmatrix} A_+ \\ A_- \end{pmatrix} = \begin{pmatrix} 0 \\ 0 \end{pmatrix}. \tag{53}$$

By taking $\det(M(\omega)) = 0$ and solving for ω, we obtain the dispersion

$$\omega_n = (\mathrm{J}^z S + B) + \tilde{t}\cos k_n. \tag{54}$$

Hence, in the case of OBC, the addition of the magnetic field and isotropic exchange increases the energy of the system by a factor of $\mathrm{J}^z S + B$. As we consider the regime in which the isotropic exchange dominates, and the amplitude of the dispersion is given by $\tilde{t} = \sqrt{t^2 - \Delta^2} < \mathrm{J}^z S + B$, the dispersion is

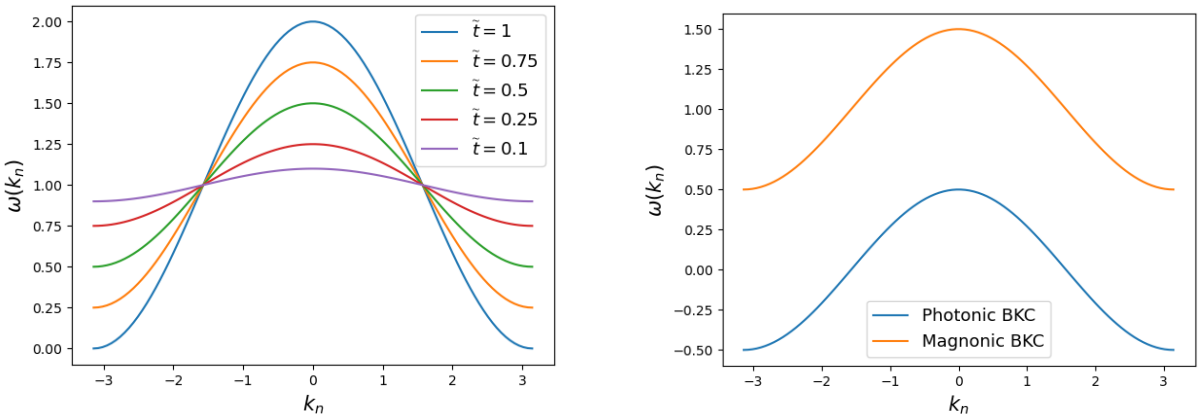

(a) (b)

Figure 13: Dispersion relation for the system with open boundary conditions. **(a)** Dispersion relation of the magnonic BKC for different values of $\tilde{t} = \sqrt{t^2 - \Delta^2}$ and $J^z S + B = 1$. We observe the characteristic dispersion of a squeezed state; the uncertainty is maximal at when the wave vector k is an integer multiple of π and minimal when it is a half-integer multiple of π. **(b)** Comparison between the dispersions of the magnonic and photonic BKC for $\tilde{t} = 0.5$ and $J^z S + B = 1$. The addition of the magnetic field and isotropic exchange shift the dispersion of the magnonic BKC which is always positive. This is in contrast to the photonic case, whose dispersion crosses zero.

now positive for any value of the wave vector k_n in contrast with the photonic case, where the dispersion is centered around zero as illustrated in Figure 13b.

Due to this shift in the dispersion relation, the excitations are no longer amplified as they propagate through the chain. As in the case of PBC, excitations propagate in the xy plane meaning that amplification –if there– takes place in the xy plane. The dominant energy terms correspond to the isotropic exchange and the magnetic field, which favour the alignment in the z direction and thus prevent the excitations from being amplified.

In order for the excitations to be amplified, we require the dispersion to become negative, that is $J^z S + B < \tilde{t}$. To determine whether or not this regime is stable, we add the Gilbert damping. Note that the new equations of motion, Eq. (46), have the same structure as Eq. (40) and thus require the same transformations. We now apply the squeezing transformation Eq. (45), the gauge transformation Eq. (48) and the standing wave ansatz Eq. (50) in the limit $\Delta = o(tN^{-\nu})$ with $\nu > 1$ to obtain the matrix equation

$$\begin{pmatrix} (\tilde{t}\cos(k_n) + (J^z S + B))(1 - i\alpha S) - \omega & 0 \\ 0 & -(\tilde{t}\cos(k_n) + (J^z S + B))(1 + i\alpha S) - \omega \end{pmatrix} \begin{pmatrix} A_+ \\ A_- \end{pmatrix} = \begin{pmatrix} 0 \\ 0 \end{pmatrix}. \tag{55}$$

We take the determinant of the dynamical matrix to zero and solve for ω to obtain

$$\omega_{GD} = (J^z S + B + \tilde{t}\cos k_n)\left(-i\alpha S \pm \sqrt{1 - (\alpha S)^2}\right); \tag{56}$$

$$\simeq -i\alpha S(J^z S + B + \tilde{t}\cos k_n), \tag{57}$$

where we used the fact that α is small to obtain the second line. The system is dynamically stable for $\mathrm{Im}(\omega_{GD}) < 0$, that is $J^z S + B > \tilde{t} = \sqrt{t^2 - \Delta^2}$, therefore in the regime where the hopping parameter is larger than the driving amplitude, the excitations are not amplified.

$\mathbf{t < \Delta}$

In the regime where the driving amplitude is larger than the hopping parameter, the squeezing

parameter is

$$e^{2r} = \frac{\Delta + t}{\Delta - t}. \tag{58}$$

By applying the squeezing transformation Eq. (45) to the linearised equations of motion Eq. (40) we obtain

$$\dot{\hat{\delta S}}_j^+ = \frac{\tilde{\Delta}}{2}(\delta\hat{S}_{j+1}^- + \delta\hat{S}_{j-1}^-) - i(J^z S + B)(\delta\hat{S}_j^+ \cosh(2r(j-j_0)) + \delta\hat{S}_j^- \sinh(2r(j-j_0))), \tag{59a}$$

$$\dot{\hat{\delta S}}_j^- = \frac{\tilde{\Delta}}{2}(\delta\hat{S}_{j+1}^+ + \delta\hat{S}_{j-1}^+) + i(J^z S + B)(\delta\hat{S}_j^+ \sinh(2r(j-j_0)) + (-1)^j \delta\hat{S}_j^- \cosh(2r(j-j_0))), \tag{59b}$$

where $\tilde{\Delta} = \sqrt{\Delta^2 - t^2}$. We now consider the limit of $t = o(\Delta N^{-\mu})$ with $\mu > 1$ (see Appendix C.2) and apply the standing wave ansatz Eq. (50) to get the matrix equation

$$\begin{pmatrix} -i(\omega - (J^z S + B)) & -\tilde{\Delta}\cos k_n \\ -\tilde{\Delta}\cos k_n & -i(\omega + (J^z S + B)) \end{pmatrix} \begin{pmatrix} A_+ \\ A_- \end{pmatrix} = \begin{pmatrix} 0 \\ 0 \end{pmatrix}. \tag{60}$$

We now take the determinant of the dynamical matrix to zero and solve for ω to obtain the dispersion relation of the system

$$\omega_\pm(k_n) = \pm\sqrt{(J^z S + B)^2 - \tilde{\Delta}^2 \cos^2 k_n}, \tag{61}$$

which is equivalent to Eq. (44) for $t = 0$. As so, Figure 14 shows that there are two energy bands which touch in the limit $J^z S + B = \tilde{\Delta}$ where we observe type-I Weyl nodes at the center and edges of the first Brillouin zone [20].

Next, we add the Gilbert damping to determine the regime of stability. To do so, we apply the squeezing

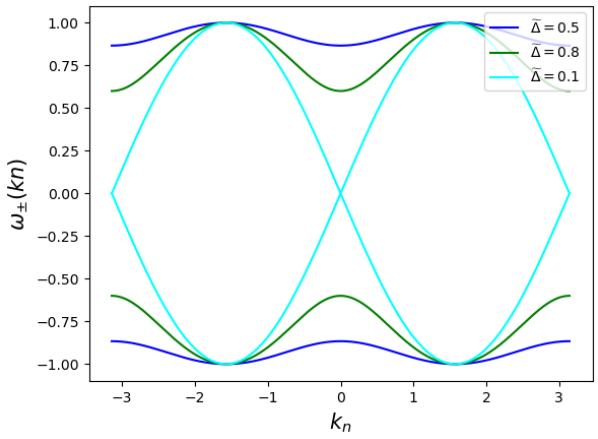

Figure 14: Dispersion relation of the system with OBC for $J^z S + B = 1$ and different values of $\tilde{\Delta}$.

transformation with parameter r defined in Eq. (58) and the standing wave ansatz Eq. (50) to the damped equations of motion Eq. (46). By writting the transformed equations of motion in matrix form we get

$$\begin{pmatrix} i(J^z S + B)(1 - i\alpha S) - i\omega & -\tilde{\Delta}\cos k_n(1 - i\alpha S) \\ -\tilde{\Delta}\cos k_n(1 + i\alpha S) & -i(J^z S + B)(1 + i\alpha S) - i\omega \end{pmatrix} \begin{pmatrix} A_+ \\ A_- \end{pmatrix} = \begin{pmatrix} 0 \\ 0 \end{pmatrix}. \tag{62}$$

We take the determinant to zero, and we have

$$\omega_\pm^{GD}(k_n) = -i\alpha S(J^z S + B) \pm \sqrt{(J^z S + B)^2 - \tilde{\Delta}^2 \cos^2 k_n (1 + (\alpha S)^2)}. \tag{63}$$

The system is dynamically stable when $\mathrm{Im}(\omega_\pm^{GD}) < 0$. Although this is always true for the negative root, $\mathrm{Im}(\omega_+^{GD}) < 0$ requires $J^z S + B > \tilde{\Delta}$, meaning that for the system to be stable, the isotropic exchange and the magnetic field must be the dominant terms.

6 The spin spiral chain

We now study the dynamics of the spin waves in the spin spiral chain Figure 3. To do so, we consider the regime where the anisotropic exchange dominates and no magnetic field is added to the system. We then compute the equations of motion and dispersion relation for the chain with PBC to compare the exitations' dynamics to these in the BKC.

6.1 Equations of motion

Since the two Hamiltonians differ only by a phase of $\pi/2$, the dynamics of the two models are the same. We thus start by computing the equations of motion in both situations and then examine them simultaneously.

6.1.1 Spin spiral chain 1

The Heisenberg equations of motion for the spin spiral chain 1 (Figure 3a) are given by

$$\dot{\hat{S}}_j^x = \frac{t+\Delta}{2S}\hat{S}_j^z\hat{S}_{j-1}^x - \frac{t-\Delta}{2S}\hat{S}_{j+1}^x\hat{S}_j^z + \frac{J^z}{2}(\hat{S}_{j+1}^z + \hat{S}_{j-1}^z)\left(S\cos\frac{3\pi}{2}j + \hat{S}_j^y\sin^2\frac{3\pi}{2}j\right), \tag{64a}$$

$$\dot{\hat{S}}_j^y = \frac{t-\Delta}{2S}\hat{S}_j^z\hat{S}_{j-1}^y - \frac{t+\Delta}{2S}\hat{S}_{j+1}^y\hat{S}_j^z - \frac{J^z}{2}(\hat{S}_{j+1}^z + \hat{S}_{j-1}^z)\left(-S\sin\frac{3\pi}{2}j + \hat{S}_j^x\cos^2\frac{3\pi}{2}j\right), \tag{64b}$$

$$\begin{aligned}\dot{\hat{S}}_j^z = \frac{1}{2S}((t+\Delta)\hat{S}_{j+1}^y - (t-\Delta)\hat{S}_{j-1}^y)\left(S\cos\frac{3\pi}{2}j + \hat{S}_j^y\sin^2\frac{3\pi}{2}j\right) + \\ \frac{1}{2S}((t-\Delta)\hat{S}_{j+1}^x - (t+\Delta)\hat{S}_{j-1}^x)\left(-S\sin\frac{3\pi}{2}j + \hat{S}_j^x\cos^2\frac{3\pi}{2}j\right),\end{aligned} \tag{64c}$$

where we used the algebra defined in Eq. (32). Since the GS is stable and therefore does not change in time, Eq. (30a) gives the condition

$$-\dot{\hat{S}}_j^x\sin\frac{3\pi}{2}j + \dot{\hat{S}}_j^y\cos\frac{3\pi}{2}j = 0, \tag{65}$$

that is

$$\dot{\hat{S}}_j^x = 0 \quad \text{for j odd}, \tag{66a}$$

$$\dot{\hat{S}}_j^y = 0 \quad \text{for j even}. \tag{66b}$$

In order to compare the motion of the two models, it is useful to rewrite the equations of motion in terms of quadratures. Using the LHPT Eq. (31) we first obtain the equations of motion for the creation and annihilation operators

$$\begin{aligned}\dot{\hat{a}}_j = -it\hat{a}_j - \frac{i}{4}\left((t+(-1)^j\Delta)(\hat{a}_{j+1}^\dagger - \hat{a}_{j+1}) + (t-(-1)^j\Delta)(\hat{a}_{j-1}^\dagger - \hat{a}_{j-1})\right) \\ + \frac{iJ^zS}{4}(\hat{a}_{j-1}^\dagger + \hat{a}_{j+1} + \hat{a}_{j-1}^\dagger + \hat{a}_{j-1}),\end{aligned} \tag{67a}$$

$$\begin{aligned}\dot{\hat{a}}_j^\dagger = it\hat{a}_j^\dagger - \frac{i}{4}\left((t+(-1)^j\Delta)(\hat{a}_{j+1}^\dagger - \hat{a}_{j+1}) + (t-(-1)^j\Delta)(\hat{a}_{j-1}^\dagger - \hat{a}_{j-1})\right) \\ - \frac{iJ^zS}{4}(\hat{a}_{j-1}^\dagger + \hat{a}_{j+1} + \hat{a}_{j-1}^\dagger + \hat{a}_{j-1}).\end{aligned} \tag{67b}$$

We then use Eq. (3) to obtain

$$\dot{\hat{x}}_j = t\hat{p}_j - \frac{1}{2}[(t+(-1)^j\Delta)\hat{p}_{j+1} + (t-(-1)^j\Delta)\hat{p}_{j-1}], \tag{68a}$$

$$\dot{\hat{p}}_j = -t\hat{x}_j + \frac{J^zS}{2}[\hat{x}_{j+1} + \hat{x}_{j-1}]. \tag{68b}$$

6.1.2 Spin spiral chain 2

In the case of the spiral chain 2 Figure 3b, the Heisenberg equations of motion are

$$\dot{\hat{S}}_j^x = \frac{t+\Delta}{2S}\hat{S}_j^z\hat{S}_{j-1}^x - \frac{t-\Delta}{2S}\hat{S}_{j+1}^x\hat{S}_j^z + \frac{J^z}{2}(\hat{S}_{j+1}^z + \hat{S}_{j-1}^z)\left(S\sin\frac{3\pi}{2}j + \hat{S}_j^y\cos^2\frac{3\pi}{2}j\right), \tag{69a}$$

$$\dot{\hat{S}}_j^y = \frac{t-\Delta}{2S}\hat{S}_j^z\hat{S}_{j-1}^y - \frac{t+\Delta}{2S}\hat{S}_{j+1}^y\hat{S}_j^z - \frac{J^z}{2}(\hat{S}_{j+1}^z + \hat{S}_{j-1}^z)\left(S\cos\frac{3\pi}{2}j + \hat{S}_j^x\sin^2\frac{3\pi}{2}j\right), \tag{69b}$$

$$\begin{aligned}\dot{\hat{S}}_j^z = &\frac{1}{2S}((t+\Delta)\hat{S}_{j+1}^y - (t-\Delta)\hat{S}_{j-1}^y)\left(S\sin\frac{3\pi}{2}j + \hat{S}_j^y\cos^2\frac{3\pi}{2}j\right)\\ &+\frac{1}{2S}((t-\Delta)\hat{S}_{j+1}^x - (t+\Delta)\hat{S}_{j-1}^x)\left(S\cos\frac{3\pi}{2}j + \hat{S}_j^x\sin^2\frac{3\pi}{2}j\right).\end{aligned} \tag{69c}$$

The GS corresponding to Eq. (34a) yields the condition

$$\dot{\hat{S}}_j^x\cos\frac{3\pi}{2}j + \dot{\hat{S}}_j^y\sin\frac{3\pi}{2}j = 0 \tag{70}$$

which can be rewriten as

$$\dot{\hat{S}}_j^x = 0 \quad \text{for j even,} \tag{71a}$$

$$\dot{\hat{S}}_j^y = 0 \quad \text{for j odd.} \tag{71b}$$

Using Eq. (35) and Eq. (3) we get the equations of motion for the quadratures:

$$\dot{\hat{x}}_j = t\hat{p}_j - \frac{1}{2}[(t-(-1)^j\Delta)\hat{p}_{j+1} + (t+(-1)^j\Delta)\hat{p}_{j-1}], \tag{72a}$$

$$\dot{\hat{p}}_j = -t\hat{x}_j + \frac{J^zS}{2}[\hat{x}_{j+1} + \hat{x}_{j-1}]. \tag{72b}$$

6.1.3 Motion in the spin spiral chain

To see how the excitations propagate in the spiral chain 1 (respectively 2), let us start by considering the case where there is no isotropic exchange, i.e. $J^z = 0$. In this case, the equations of motion of the x and y components of the spin take a similar shape to those of the quadratures in the BKC. The two components are dynamically decoupled and they are forced in a spatially asymmetric manner by its neighbours. However, contrary to the BKC, the GS is in the xy plane, and therefore the z component of the spin is not constant, and the dynamics of both the x and y components depend on it.
From Eq. (66) (Eq. (71)) we see that the excitations do not propagate in a given plane but alternate between the xz and yz planes instead. At odd (even) sites, the spins in the ground state are in the x-direction, thus the excitations propagate in the yz plane. The dynamics of the y-component only depend on the z-component at the same site. The z-component, however, is not only coupled to the y-component, but is also forced by the x-component of the neighbouring spins as well; the left neighbour amplifies the excitation, and the right one deamplifies it.
Similarly, at even (odd) sites, the spins of the ground state are in the y-direction, therefore the excitation is in the xz plane. In this case, the x-component cuples to the z-component, which in turn is forced by the y-component of the neighbouring spins. Here, the left neighbour deamplifies the excitation while the right one amplifies it.
By dividing the chain into the two sublattices

$$\Lambda^x = \{j : \dot{\hat{S}}_j^x = 0\},$$
$$\Lambda^y = \{j : \dot{\hat{S}}_j^y = 0\},$$

what we see is that while an excitation on Λ^x is amplified as it propagates from left to right and deamplified in the opposite direction, an excitation on Λ^y exhibits the opposite behaviour; it is amplified as it propagates from right to left and deamplified when propagating from left to right. The amplification is compensated by the deamplification, meaning that the net amplification is zero.
When the isotropic exchange is added, Eq. (66) (Eq. (71)) still holds, hence the excitation propagates alternating between the xz and yz planes. The dynamics of the z-component of the spin are unchanged, however, as is the case for the BKC, the addition of the isotropic exchange dynamically couples the x and y components of the spin. By doing so, the x and y components are now forced by the z-component of the neighbouring spins in a spatially symmetric way.

Contrary to the BKC, where for $J^z = 0$ the x and y quadratures are dynamically decoupled (see Eq. (5)), in the spiral chain Eq. (68) (Eq. (72)) shows that even when there is no isotropic exchange added, the two quadratures are always dynamically coupled. Moreover, we see that the dynamics of the x quadrature only depends on the p quadrature and viceversa.
By looking at the dynamics of the x-quadrature, i.e. Eq. (68a) and Eq. (72a), we see that an excitation will be amplified and then deamplified when going through two sites independently of the direction of propagation.
To further understand the dynamics of the model, we now compute the dispersion relation focussing on the system with PBC.

6.2 Dispersion relation for periodic boundary conditions

For PBC, the two spiral GS, see Figure 3, are the same since the choice of the first spin is arbitrary. Hence, the two spiral chains are the same.
To compute the dispersion relation, we start by applying the Fourier transform

$$\hat{a}_j = \frac{1}{\sqrt{N}} \sum_k e^{ikj} \hat{a}_k \tag{73}$$

to the Hamiltonian Eq. (33a) to obtain it in the momentum space

$$\begin{aligned} \hat{H} &= \sum_k \left(t - \frac{1}{2}(t + J^z S)\cos k \right) \hat{a}_k^\dagger \hat{a}_k + \frac{1}{4}(t - J^z S) \sum_k (e^{ik} \hat{a}_{-k}^\dagger \hat{a}_k^\dagger + e^{-ik} \hat{a}_{-k} \hat{a}_k) + \\ &\frac{\Delta}{4} \sum_k (e^{i(k-\pi)} (\hat{a}_{-k+\pi}^\dagger \hat{a}_k^\dagger - \hat{a}_k^\dagger \hat{a}_{k-\pi}) + e^{-i(k+\pi)} (\hat{a}_{-k-\pi} \hat{a}_k - \hat{a}_{k+\pi}^\dagger \hat{a}_k)), \\ &= \sum_k \vec{\alpha}^\dagger \underline{\mathcal{H}} \vec{\alpha}, \end{aligned} \tag{74}$$

where we defined the vector $\vec{\alpha}^\dagger = (\hat{a}_{k+\pi}^\dagger, \hat{a}_k^\dagger, \hat{a}_{-k-\pi}^\dagger, \hat{a}_{-k}^\dagger, \hat{a}_{-k+\pi}^\dagger, \hat{a}_{k+\pi}, \hat{a}_k, \hat{a}_{-k-\pi}, \hat{a}_{-k}, \hat{a}_{-k+\pi})$, and the matrix

$$\underline{\mathcal{H}} = \begin{pmatrix} 0 & -\frac{\Delta}{4} e^{-i(k+\pi)} & 0 & 0 & 0 & 0 & 0 & 0 & 0 & 0 & 0 & 0 \\ 0 & t - \frac{t+J^z S}{2} \cos k & -\frac{\Delta}{4} e^{i(k-\pi)} & 0 & 0 & 0 & 0 & 0 & 0 & 0 & 0 & 0 \\ 0 & 0 & 0 & 0 & 0 & 0 & 0 & 0 & 0 & 0 & 0 & 0 \\ 0 & 0 & 0 & 0 & 0 & 0 & 0 & 0 & 0 & 0 & 0 & 0 \\ 0 & 0 & 0 & 0 & 0 & 0 & 0 & \frac{t-J^z S}{4} e^{ik} & 0 & 0 & 0 & 0 \\ 0 & 0 & 0 & 0 & 0 & 0 & 0 & \frac{\Delta}{4} e^{i(k-\pi)} & 0 & 0 & 0 & 0 \\ 0 & 0 & 0 & 0 & 0 & 0 & 0 & 0 & 0 & 0 & 0 & 0 \\ 0 & 0 & 0 & 0 & 0 & 0 & 0 & 0 & 0 & 0 & 0 & 0 \\ 0 & 0 & 0 & 0 & 0 & 0 & 0 & 0 & 0 & 0 & 0 & 0 \\ 0 & \frac{\Delta}{4} e^{-i(k+\pi)} & 0 & 0 & 0 & 0 & 0 & 0 & 0 & 0 & 0 & 0 \\ 0 & \frac{t-J^z S}{4} e^{-ik} & 0 & 0 & 0 & 0 & 0 & 0 & 0 & 0 & 0 & 0 \\ 0 & 0 & 0 & 0 & 0 & 0 & 0 & 0 & 0 & 0 & 0 & 0 \end{pmatrix}.$$

Next, we consider the matrix

$$\underline{\Gamma} = \begin{pmatrix} \mathbb{1}_6 & 0 \\ 0 & -\mathbb{1}_6 \end{pmatrix}. \tag{75}$$

to obtain the dynamical matrix $M(\omega) = \underline{\mathcal{H}} - \omega(k)\underline{\Gamma}$ [21]. The dispersion relation is then obtained by taking the determinant of the dynamical matrix to zero and solving for ω, which yields

$$\omega(k) = t - \frac{1}{2}(t + \mathrm{J}^z S)\cos k. \tag{76}$$

We remark that the dispersion is independent of the driving amplitude Δ, which reflects the fact that when an excitation propagates through the chain, any amplification is compensated with deamplification. Thus, the excitation does not feel the effect of the symmetric anisotropic exchange. Moreover, since ω is always real, the system is always dynamically stable. Figure 15 shows the dispersion relation of the

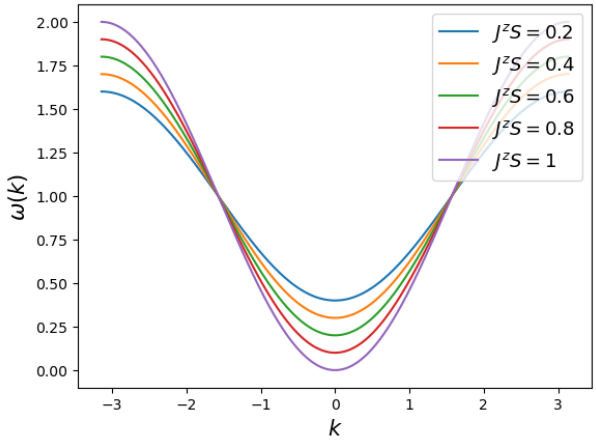

Figure 15: Dispersion relation as a function of the wavevector k for different values of the isotropic exchange parameter and $t = 1$.

system for different values of $\mathrm{J}^z S$. We recognise the characteristic shape of the dispersion relation of a squeezed state[22, 23]. This corresponds to a two-mode squeezed state with squeezing parameter to be determined.

7 Conclusion

In this thesis, we have defined a spin Hamiltonian with a non-trivial topology that has two stable phases, which depend on the dominant energy contribution and the presence or lack of a magnetic field in the z-direction. After determining the ground state, we have used a linear Holstein-Primakkof transformation to determine the dynamics of the excitations in the system. In the regime where the isotropic exchange dominates, the spins are aligned in the z-direction, and the system behaves as the BKC. Hence, in this regime the spin Hamiltonian Eq. (6) defines the magnonic BKC. Then, in the regime where the anisotropic exchange dominates and no magnetic field is added to the system, the ground state is given by a periodic, non-collinear missalignment of the spins in the xy plane.
Although we have defined a magnonic BKC, this does not show any amplification of spin waves. The spin waves propagate in the xy plane while the equilibrium configuration corresponds to the ferromagnetic alignment of spins in the z-direction. In order for the system to be in the equilibrium state, the isotropic exchange must dominate over the anisotropic one, meaning that any amplification will be damped by the isotropic exchange.
In order to obtain amplification, we should require that the magnetic field cancels out the effect of the isotropic exchange, i.e. $B = -\mathrm{J}^z S$. However in this case, the system becomes dynamically unstable.

A Algebra

$$[\hat{S}_j^+, \hat{S}_{j'}^-] = [\sqrt{2S}\hat{a}_j, \sqrt{2S}\hat{a}_{j'}^\dagger], \tag{77}$$
$$= 2S[\hat{a}_j, \hat{a}_{j'}^\dagger], \tag{78}$$
$$= 2S\delta_{j,j'}. \tag{79}$$

$$[\hat{S}_j^z, \hat{S}_{j'}^+] = [S - \hat{a}_j^\dagger \hat{a}_j, \sqrt{2S}\hat{a}_{j'}], \tag{80}$$
$$= -\sqrt{2S}[\hat{a}_j^\dagger \hat{a}_j, \hat{a}_{j'}], \tag{81}$$
$$= \sqrt{2S}\hat{a}_j\delta_{j,j'}, \tag{82}$$
$$= \hat{S}_j^+\delta_{j,j'}. \tag{83}$$

$$[\hat{S}_j^z, \hat{S}_{j'}^-] = [S - \hat{a}_j^\dagger \hat{a}_j, \sqrt{2S}\hat{a}_{j'}^\dagger], \tag{84}$$
$$= -\sqrt{2S}[\hat{a}_j^\dagger \hat{a}_j, \hat{a}_{j'}^\dagger], \tag{85}$$
$$= -\sqrt{2S}\hat{a}_j^\dagger\delta_{j,j'}, \tag{86}$$
$$= -\hat{S}_j^-\delta_{j,j'}. \tag{87}$$

B Squeeze operator

In order to compute the dispersion relation of our system, we first need to define the spin squeeze operator and its action on the spin components, which can be done in analogy to the squeze operator of the one-dimensional harmonic oscillator [24]. In the case of the photonic BKC, the squeeze operator is given by

$$\hat{U}(r) = e^{r(j-j_0)((\hat{a}_j)^2 - (\hat{a}_j^\dagger)^2)}, \tag{88}$$

where r is characterized by Eq. (47) and j_0 is an arbitrary real number. Since the second quantization operators are related to the bosonic spin ladder operators through the linear Holstein-Primakoff transformation Eq. (26), it is easy to see that we can approximate the squeeze operator by

$$\hat{U}_j(r) = exp\left(\frac{-r(j-j_0)}{4S}((\hat{S}_j^-)^2 - (\hat{S}_j^+)^2)\right). \tag{89}$$

In general, it is not easy to define the action of the squeeze operator due to the algebra of the spins, however, due to the "simplified" algebra that arises from the LHPT, we will show that the spin squeeze operator acts in analogy to the photonic one when acting on the x and y components of the spin.
First let us look at the following commutators:

$$[(\hat{S}_j^-)^2 - (\hat{S}_j^+)^2, \hat{S}_{j'}^+] = -4S\hat{S}_j^-\delta_{j,j'}, \tag{90}$$
$$[(\hat{S}_j^-)^2 - (\hat{S}_j^+)^2, \hat{S}_{j'}^-] = -4S\hat{S}_j^+\delta_{j,j'}, \tag{91}$$
$$[(\hat{S}_j^-)^2 - (\hat{S}_j^+)^2, \hat{S}_{j'}^z] = 2S((\hat{S}_j^-)^2 + (\hat{S}_j^+)^2)\delta_{j,j'}, \tag{92}$$
$$[(\hat{S}_j^-)^2 - (\hat{S}_j^+)^2, [(\hat{S}_{j'}^-)^2 - (\hat{S}_{j'}^+)^2, \hat{S}_{j'}^z]] = -16S(\hat{S}_j^+\hat{S}_j^- + \hat{S}_j^-\hat{S}_j^+)\delta_{j,j'}. \tag{93}$$

We now apply the commutator k times:

$$[\xi_j((\hat{S}_j^-)^2 - (\hat{S}_j^+)^2), [\xi_j((\hat{S}_j^-)^2 - (\hat{S}_j^+)^2), ..., [\xi_j((\hat{S}_j^-)^2 - (\hat{S}_j^+)^2), \hat{S}_j^+]...]] = \begin{cases} (4S\xi_j)^k\hat{S}_j^+ & \text{for k even,} \\ -(4S\xi_j)^k\hat{S}_j^- & \text{for k odd,} \end{cases}$$

$$[\xi_j((\hat{S}_j^-)^2-(\hat{S}_j^+)^2),[\xi_j((\hat{S}_j^-)^2-(\hat{S}_j^+)^2),...,[\xi_j((\hat{S}_j^-)^2-(\hat{S}_j^+)^2),\hat{S}_j^-]...]] = \begin{cases}(4S\xi_j)^k\hat{S}_j^- & \text{for k even,}\\ -(4S\xi_j)^k\hat{S}_j^+ & \text{for k odd,}\end{cases}$$

$$[\xi_j((\hat{S}_j^-)^2-(\hat{S}_j^+)^2),...,[\xi_j((\hat{S}_j^-)^2-(\hat{S}_j^+)^2),\hat{S}_j^z]...]] = \begin{cases}-(4S)^{k-1}(2\xi_j)^k(\hat{S}_j^+\hat{S}_j^- + \hat{S}_j^-\hat{S}_j^+) & \text{for k even,}\\ (4S)^{k-1}(2\xi_j)^k((\hat{S}_j^-)^2+(\hat{S}_j^+)^2) & \text{for k odd,}\end{cases}$$

where $\xi_j := r(j-j_0)/4S$.

C Limits

C.1 Limit $\Delta \ll t$

In order to be able to perform the Taylor expansion that allow us to get rid of the site-dependence in Eq. (49), we require $2r(j-j_0) \ll 1$ for any j_0 and j. In particular, since both $\cosh(x)$ and $\sinh(x)$ are increasing functions of x, we require $\max_{j\in[1,N]}\{2r(j-j_0)\} = 2r(N-j_0) \ll 1$ for any j_0. We have $e^{2r} = \frac{t+\Delta}{t-\Delta} \approx 1$ when $\Delta \ll t$, so we define $\Delta = t/N^\nu$ leading to $2r(N-j_0) = (N-j_0)\ln(1+2/(N^\nu-1))$. Since we want to look at the limit of N going to infinity we have $N-j_0 \approx N$, and for $\nu \geq 1$, $N^\nu - 1 \approx N^\nu$. By defining $x = 1/N$ we obtain

$$\lim_{x\to 0}\frac{1}{x}\ln(1+2x^\nu) = \frac{0}{0}, \tag{95}$$

$$= \lim_{x\to 0}\frac{2\nu x^{\nu-1}}{1+2x^\nu} = 0 \quad \text{for } \nu > 1. \tag{96}$$

We conclude that $\forall j, j_0 \in [1,N]$, $\cosh(2r(j-j_0)) \approx 1$ and $\sinh(2r(j-j_0)) \approx 0$ hold for $\Delta = o(t/N^\nu)$ with $\nu > 1$.

C.2 Limit $t \ll \Delta$

As in the case where the hopping parameter is large in front of the driving amplitude, in order to determine the dispersion relation of the system we must have $\max_{j\in[1,N]}\{2r(j-j_0)\} = 2r(N-j_0) \ll 1$ for any j_0. We have $e^{2r} = \frac{\Delta+t}{\Delta-t} \approx 1$ when $t \ll \Delta$, so we define $t = \Delta/N^\mu$ leading to $2r(N-j_0) = (N-j_0)\ln(1+2/(N^\mu-1))$.
Since we want to look at the limit of N going to infinity we have $N-j_0 \approx N$, and for $\mu \geq 1$, $N^\mu - 1 \approx N^\mu$. By defining $x = 1/N$ we obtain

$$\lim_{x\to 0}\frac{1}{x}\ln(1+2x^\mu) = \frac{0}{0}, \tag{97}$$

$$= \lim_{x\to 0}\frac{2\mu x^{\mu-1}}{1+2x^\mu} = 0 \quad \text{for } \mu > 1. \tag{98}$$

Hence, $\forall j, j_0 \in [1,N]$, $\cosh(2r(j-j_0)) \approx 1$ and $\sinh(2r(j-j_0)) \approx 0$ hold for $t = o(\Delta/N^\mu)$ with $\mu > 1$.

D Second order HPT around the FM GS

If we now consider the second order terms in the LHPT around the FM ground state, Eq. (26) now becomes

$$\hat{S}_j^z = S - \hat{a}_j^\dagger\hat{a}_j, \tag{99a}$$

$$\hat{S}_j^+ = \hat{S}_j^x + i\hat{S}_j^y \simeq \sqrt{2S}\left(1 - \frac{\hat{a}_j^\dagger \hat{a}_j}{4S}\right)\hat{a}_j, \tag{99b}$$

$$\hat{S}_j^- = \hat{S}_j^x - i\hat{S}_j^y \simeq \sqrt{2S}\hat{a}_j^\dagger\left(1 - \frac{\hat{a}_j^\dagger \hat{a}_j}{4S}\right). \tag{99c}$$

By plugging it into the spin Hamiltonian Eq. (6), we obtain

$$\begin{aligned}\hat{H} = \hat{H}_0 &+ \frac{it}{8S}\sum_j (2\hat{a}_{j+1}^\dagger \hat{a}_j + \hat{a}_{j+1}^\dagger \hat{a}_{j+1}(\hat{a}_{j+1}\hat{a}_j^\dagger - \hat{a}_{j+1}^\dagger \hat{a}_j) + (\hat{a}_{j+1}\hat{a}_j^\dagger - \hat{a}_{j+1}^\dagger \hat{a}_j)\hat{a}_j^\dagger \hat{a}_j) \\ &- \frac{i\Delta}{8S}\sum_j (\hat{a}_{j+1}\hat{a}_j - \hat{a}_{j+1}^\dagger \hat{a}_j^\dagger + \hat{a}_{j+1}^\dagger \hat{a}_{j+1}(\hat{a}_{j+1}^\dagger \hat{a}_j^\dagger - \hat{a}_{j+1}\hat{a}_j) + (\hat{a}_{j+1}^\dagger \hat{a}_j^\dagger - \hat{a}_{j+1}\hat{a}_j)\hat{a}_j^\dagger \hat{a}_j) \\ &- \frac{J^z}{2}\hat{a}_{j+1}^\dagger \hat{a}_{j+1}\hat{a}_j^\dagger \hat{a}_j,\end{aligned} \tag{100}$$

where $\hat{H}_0$ denotes the lowest order Hamiltonian defined in Eq. (29). We see that in this case the excitations no longer behave as the excitations of the BKC. At second order we lose the asymmetry that characterizes the BKC even in the limit $J^z S + B = 0$.

References

[1] Frédéric Chazal and Bertrand Michel. An introduction to topological data analysis: fundamental and practical aspects for data scientists. *Frontiers in Artificial Intelligence*, 4:108, 2021.

[2] Henry Adams and Michael Moy. Topology applied to machine learning: From global to local. *Frontiers in Artificial Intelligence*, 4:668302, 2021.

[3] Luca Tubiana, Gareth P Alexander, Agnese Barbensi, Dorothy Buck, Julyan HE Cartwright, Mateusz Chwastyk, Marek Cieplak, Ivan Coluzza, Simon Čopar, David J Craik, et al. Topology in soft and biological matter. *Physics Reports*, 1075:1–137, 2024.

[4] Qian Niu, Ds J Thouless, and Yong-Shi Wu. Quantized hall conductance as a topological invariant. *Physical Review B*, 31(6):3372, 1985.

[5] David R Nelson and JM Kosterlitz. Universal jump in the superfluid density of two-dimensional superfluids. *Physical Review Letters*, 39(19):1201, 1977.

[6] John M Kosterlitz and DJ Thouless. Long range order and metastability in two dimensional solids and superfluids.(application of dislocation theory). *Journal of Physics C: Solid State Physics*, 5(11):L124, 1972.

[7] John Michael Kosterlitz and David James Thouless. Ordering, metastability and phase transitions in two-dimensional systems. In *Basic Notions Of Condensed Matter Physics*, pages 493–515. CRC Press, 2018.

[8] F Duncan M Haldane. Nonlinear field theory of large-spin heisenberg antiferromagnets: semi-classically quantized solitons of the one-dimensional easy-axis néel state. *Physical review letters*, 50(15):1153, 1983.

[9] F Duncan M Haldane. Model for a quantum hall effect without landau levels: Condensed-matter realization of the" parity anomaly". *Physical review letters*, 61(18):2015, 1988.

[10] JM Kosterlitz, D Haldane, and DJ Thouless. Topological phase transitions and topological phases of matter. *Scientific Background on the Nobel Prize in Physics*, 2016.

[11] Masatoshi Sato and Yoichi Ando. Topological superconductors: a review. *Reports on Progress in Physics*, 80(7):076501, 2017.

[12] Michael I Monastyrsky. *Topology in condensed matter*, volume 150. Springer Science & Business Media, 2006.

[13] A Yu Kitaev. Unpaired majorana fermions in quantum wires. *Physics-uspekhi*, 44(10S):131, 2001.

[14] Haining Pan and Sankar Das Sarma. Majorana nanowires, kitaev chains, and spin models. *Physical Review B*, 107(3):035440, 2023.

[15] R Baquero. Brief introduction to superconductivity. *Departamento de Física, Cinvestav*, 2005.

[16] Alexander McDonald, T Pereg-Barnea, and AA Clerk. Phase-dependent chiral transport and effective non-hermitian dynamics in a bosonic kitaev-majorana chain. *Physical Review X*, 8(4):041031, 2018.

[17] Ulf Leonhardt. *Essential quantum optics: from quantum measurements to black holes*. Cambridge University Press, 2010.

[18] Theodore Holstein and Henry Primakoff. Field dependence of the intrinsic domain magnetization of a ferromagnet. *Physical Review*, 58(12):1098, 1940.

[19] A Roldán-Molina, MJ Santander, AS Núnez, and Joaquín Fernández-Rossier. Quantum theory of spin waves in finite chiral spin chains. *Physical Review B*, 89(5):054403, 2014.

[20] Viktor Könye, Corentin Morice, Dmitry Chernyavsky, Ali G Moghaddam, Jeroen van Den Brink, and Jasper van Wezel. Horizon physics of quasi-one-dimensional tilted weyl cones on a lattice. *Physical Review Research*, 4(3):033237, 2022.

[21] JHP Colpa. Diagonalization of the quadratic boson hamiltonian. *Physica A: Statistical Mechanics and its Applications*, 93(3-4):327–353, 1978.

[22] Gilbert Grynberg, Alain Aspect, and Claude Fabre. *Introduction to quantum optics: from the semi-classical approach to quantized light*. Cambridge university press, 2010.

[23] David J Wineland, John J Bollinger, Wayne M Itano, FL Moore, and Daniel J Heinzen. Spin squeezing and reduced quantum noise in spectroscopy. *Physical Review A*, 46(11):R6797, 1992.

[24] Mehdi Miri and Sina Khorasani. Displacement and squeeze operators of a three-dimensional harmonic oscillator and their associated quantum states. *arXiv preprint arXiv:0912.3335*, 2009.